

SCALABLE ONE-PASS OPTIMISATION OF HIGH-DIMENSIONAL WEIGHT-UPDATE HYPERPARAMETERS BY IMPLICIT DIFFERENTIATION

Ross M. Clarke
University of Cambridge
rmc78@cam.ac.uk

Elre T. Oldewage
University of Cambridge
etv21@cam.ac.uk

José Miguel Hernández-Lobato
University of Cambridge
Alan Turing Institute
jmh233@cam.ac.uk

ABSTRACT

Machine learning training methods depend plentifully and intricately on hyperparameters, motivating automated strategies for their optimisation. Many existing algorithms restart training for each new hyperparameter choice, at considerable computational cost. Some hypergradient-based one-pass methods exist, but these either cannot be applied to arbitrary optimiser hyperparameters (such as learning rates and momenta) or take several times longer to train than their base models. We extend these existing methods to develop an approximate hypergradient-based hyperparameter optimiser which is applicable to any continuous hyperparameter appearing in a differentiable model weight update, yet requires only one training episode, with no restarts. We also provide a motivating argument for convergence to the true hypergradient, and perform tractable gradient-based optimisation of independent learning rates for each model parameter. Our method performs competitively from varied random hyperparameter initialisations on several UCI datasets and Fashion-MNIST (using a one-layer MLP), Penn Treebank (using an LSTM) and CIFAR-10 (using a ResNet-18), in time only 2–3x greater than vanilla training.

1 INTRODUCTION

Many machine learning methods are governed by *hyperparameters*: quantities which, unlike model *parameters* or *weights*, control the training process itself (e.g. optimiser settings, dropout probabilities and dataset configurations). As suitable hyperparameter selection is crucial to system performance (e.g. Kohavi & John (1995)), it is a pillar of efforts to automate machine learning (Hutter et al., 2018, Chapter 1), spawning several hyperparameter optimisation (HPO) algorithms (e.g. Bergstra & Bengio (2012); Snoek et al. (2012; 2015); Falkner et al. (2018)). However, HPO is computationally intensive and random search is an unexpectedly strong baseline (but beatable; Turner et al. (2021)); beyond random or grid searches, HPO is relatively underused in research (Bouthillier & Varoquaux, 2020).

Recently, Lorraine et al. (2019) used gradient-based updates to adjust hyperparameters *during* training, displaying impressive optimisation performance and scalability to high-dimensional hyperparameters. Despite their computational efficiency (since updates occur before final training performance is known), Lorraine et al.’s algorithm only applies to hyperparameters on which the loss function depends explicitly (such as ℓ_2 regularisation), notably excluding optimiser hyperparameters.

Our work extends Lorraine et al.’s algorithm to support arbitrary continuous inputs to a differentiable weight update formula, including learning rates and momentum factors. We demonstrate our algorithm handles a range of hyperparameter initialisations and datasets, improving test loss after a single training episode (‘one pass’). Relaxing differentiation-through-optimisation (Domke, 2012) and hypergradient descent’s (Baydin et al., 2018) exactness allows us to improve computational and memory efficiency. Our scalable one-pass method improves performance from arbitrary hyperparameter initialisations, and could be augmented with a further search over those initialisations if desired.

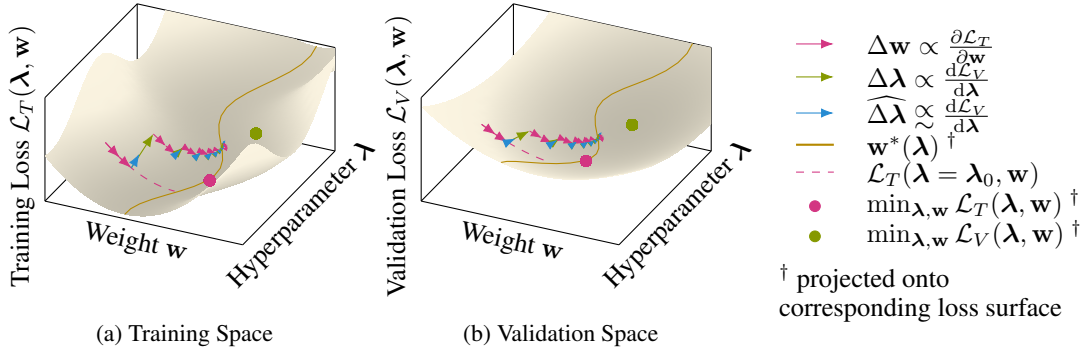


Figure 1: Summary of our derivation (Section 2): sample online hypergradient descent using exact hypergradients from the implicit function theorem (IFT) (\rightarrow), with our method’s approximate hypergradients (\rightarrow) superimposed. We target optimal validation loss (\bullet), adjusting weights \mathbf{w} based on the training loss. Classical weight updates (for fixed hyperparameters λ) converge (\rightarrow , $---$) to the best-response line $\mathbf{w}^*(\lambda)$ ($---$); the IFT gives hyperparameter updates (\rightarrow) leading to a minimum of validation loss along $\mathbf{w}^*(\lambda)$. Our approximate hyperparameter updates (\rightarrow) differ in magnitude from these exact updates, but still give useful guidance.

2 WEIGHT-UPDATE HYPERPARAMETER TUNING

In this section, we develop our method. Expanded derivations and a summary of differences from Lorraine et al. (2019) are given in Appendix C.

2.1 IMPLICIT FUNCTION THEOREM IN BILEVEL OPTIMISATION

Consider some model with learnable parameters \mathbf{w} , training loss \mathcal{L}_T , optimisation hyperparameters λ and validation loss \mathcal{L}_V . We use \mathbf{w}^* , λ^* to represent the optimal values of these quantities, found by solving the following *bilevel optimisation problem*:

$$\text{(a) } \lambda^* = \arg \min_{\lambda} \mathcal{L}_V(\lambda, \mathbf{w}^*(\lambda)), \quad \text{such that} \quad \text{(b) } \mathbf{w}^*(\lambda) = \arg \min_{\mathbf{w}} \mathcal{L}_T(\lambda, \mathbf{w}). \quad (1)$$

The optimal model parameters \mathbf{w}^* may vary with λ , making \mathcal{L}_V an *implicit* function of λ alone.

We approach the outer optimisation (1a) similarly to Lorraine et al. (2019) and Majumder et al. (2019), using the *hypergradient*: the total derivative of \mathcal{L}_V with respect to the hyperparameters λ . One strategy for solving (1) is therefore to alternate between updating \mathbf{w} for several steps using $\frac{\partial \mathcal{L}_T}{\partial \mathbf{w}}$ and updating λ using the hypergradient, as shown in Figure 1 (by \rightarrow and \rightarrow).

Carefully distinguishing the total differential $d\lambda$ and the partial differential $\partial\lambda$, we have

$$\frac{d\mathcal{L}_V}{d\lambda} = \frac{\partial \mathcal{L}_V}{\partial \lambda} + \frac{\partial \mathcal{L}_V}{\partial \mathbf{w}^*} \frac{\partial \mathbf{w}^*}{\partial \lambda}. \quad (2)$$

While derivatives of \mathcal{L}_V are easily computed for typical loss functions, the final derivative of the optimal model parameters ($\frac{\partial \mathbf{w}^*}{\partial \lambda}$) presents some difficulty. Letting square brackets indicate the evaluation of the interior at the subscripted values, we may rewrite $\frac{\partial \mathbf{w}^*}{\partial \lambda}$ as follows:

Theorem 1 (Cauchy’s Implicit Function Theorem (IFT)) *Suppose for some λ' and \mathbf{w}' that $[\frac{\partial \mathcal{L}_T}{\partial \mathbf{w}}]_{\lambda', \mathbf{w}'} = \mathbf{0}$. If $\frac{\partial \mathcal{L}_T}{\partial \mathbf{w}}$ is a continuously differentiable function with invertible Jacobian, then there exists a function $\mathbf{w}^*(\lambda)$ over an open subset of hyperparameter space, such that λ' lies in the open subset, $[\frac{\partial \mathcal{L}_T}{\partial \mathbf{w}}]_{\lambda, \mathbf{w}^*(\lambda)} = \mathbf{0}$ and*

$$\frac{\partial \mathbf{w}^*}{\partial \lambda} = - \left(\frac{\partial^2 \mathcal{L}_T}{\partial \mathbf{w} \partial \mathbf{w}^\top} \right)^{-1} \frac{\partial^2 \mathcal{L}_T}{\partial \mathbf{w} \partial \lambda^\top}. \quad (3)$$

$\mathbf{w}^*(\lambda)$ is called the *best response* of \mathbf{w} to λ (Figure 1). While (3) suggests a route to computing $\frac{\partial \mathbf{w}^*}{\partial \lambda}$, inverting a potentially high-dimensional Hessian in \mathbf{w} is not computationally tractable.

2.2 APPROXIMATE BEST-RESPONSE DERIVATIVE

To develop and justify a computationally tractable approximation to (3), we mirror the strategy of Lorraine et al. (2019). Consider the broad class of weight optimisers with updates of the form

$$\mathbf{w}_i(\boldsymbol{\lambda}) = \mathbf{w}_{i-1}(\boldsymbol{\lambda}) - \mathbf{u}(\boldsymbol{\lambda}, \mathbf{w}_{i-1}(\boldsymbol{\lambda})) \quad (4)$$

for some arbitrary differentiable function \mathbf{u} , with i indexing each update iteration. We deviate here from the approach of Lorraine et al. (2019) by admitting general functions $\mathbf{u}(\boldsymbol{\lambda}, \mathbf{w})$, rather than assuming the particular choice $\mathbf{u}_{\text{SGD}} = \eta \frac{\partial \mathcal{L}_T}{\partial \mathbf{w}}$. In particular, this allows $\boldsymbol{\lambda}$ to include optimiser hyperparameters. Differentiating (4) and unrolling the recursion gives

$$\left[\frac{\partial \mathbf{w}_i}{\partial \boldsymbol{\lambda}} \right]_{\boldsymbol{\lambda}'} = - \sum_{0 \leq j < i} \left(\prod_{k \leq j} \left[\mathbf{I} - \frac{\partial \mathbf{u}}{\partial \mathbf{w}} \right]_{\boldsymbol{\lambda}', \mathbf{w}_{i-1-k}} \right) \left[\frac{\partial \mathbf{u}}{\partial \boldsymbol{\lambda}} \right]_{\boldsymbol{\lambda}', \mathbf{w}_{i-1-j}}, \quad (5)$$

where j indexes our steps back through time from \mathbf{w}_{i-1} to \mathbf{w}_0 , and all \mathbf{w} depend on the current hyperparameters $\boldsymbol{\lambda}'$ — see Appendix C.2 for the full derivation. Now, we follow Lorraine et al. and assume $\mathbf{w}_0, \dots, \mathbf{w}_{i-1}$ to be equal to \mathbf{w}_i . With this, we simplify the product in (5) to a j th power by evaluating all derivatives at \mathbf{w}_i . This result is then used to approximate $\frac{\partial \mathbf{w}^*}{\partial \boldsymbol{\lambda}}$ by further assuming that $\mathbf{w}_i \approx \mathbf{w}^*$. These two approximations lead to

$$\left[\frac{\partial \mathbf{w}_i}{\partial \boldsymbol{\lambda}} \right]_{\boldsymbol{\lambda}'} \approx - \left[\sum_{0 \leq j < i} \left(\mathbf{I} - \frac{\partial \mathbf{u}}{\partial \mathbf{w}} \right)^j \frac{\partial \mathbf{u}}{\partial \boldsymbol{\lambda}} \right]_{\boldsymbol{\lambda}', \mathbf{w}_i(\boldsymbol{\lambda}')} \approx \left[\frac{\partial \mathbf{w}^*}{\partial \boldsymbol{\lambda}} \right]_{\boldsymbol{\lambda}'}. \quad (6)$$

We reinterpret i as a predefined look-back distance, trading off accuracy and computational efficiency.

These approximations actually combine to give $\mathbf{w}_i = \mathbf{w}^*$ for all i , which is initially inaccurate, but as training proceeds we would expect it to become more correct. In mitigation, we perform several weight updates prior to each hyperparameter update. This means derivatives in earlier terms of the series of (6) (which are likely the largest, dominant terms) are evaluated at weights closer to \mathbf{w}^* , therefore making the summation more accurate. In Section 4, we show that the approximations described here result in an algorithm that is both practical and effective.

Our approximate result (6) combines the general weight update of Majumder et al. (2019) with the overall approach and constant-weight assumption of Lorraine et al. (2019). The latter empirically show that an approximation similar to (6) leads to a directionally-accurate approximate hypergradient; we illustrate the approximate updates from our derivations in Figure 1 (by \rightarrow).

2.3 CONVERGENCE TO BEST-RESPONSE DERIVATIVE

To justify the approximations in (6), note that the central part of that equation is a truncated Neumann series. Taking the limit $i \rightarrow \infty$, when such a limit exists, results in the closed form

$$\left[\frac{\partial \mathbf{w}^*}{\partial \boldsymbol{\lambda}} \right]_{\boldsymbol{\lambda}'} \approx - \left[\left(\frac{\partial \mathbf{u}}{\partial \mathbf{w}} \right)^{-1} \frac{\partial \mathbf{u}}{\partial \boldsymbol{\lambda}} \right]_{\boldsymbol{\lambda}', \mathbf{w}^*(\boldsymbol{\lambda}')}. \quad (7)$$

This is precisely the result of the IFT (Theorem 1) applied to \mathbf{u} instead of $\frac{\partial \mathcal{L}_T}{\partial \mathbf{w}}$; that is, substituting the simple SGD update $\mathbf{u}_{\text{SGD}}(\boldsymbol{\lambda}, \mathbf{w}) = \eta \frac{\partial \mathcal{L}_T}{\partial \mathbf{w}}$ into (7) recovers (3) exactly. Thus, under certain conditions, our approximation (6) converges to the true best-response Jacobian in the limit of infinitely long look-back windows.

2.4 HYPERPARAMETER UPDATES

Substituting (6) into (2) yields a tractable approximation for the hypergradient $\frac{d\mathcal{L}_V}{d\boldsymbol{\lambda}}$, with which we can update hyperparameters by gradient descent. Our implementation in Algorithm 1, Figure 4, closely parallels Lorraine et al.’s algorithm, invoking Jacobian-vector products (Pearlmutter, 1994) during gradient computation for memory efficiency via the `grad_outputs` argument, which also provides the repeated multiplication for the j th power in (6). Thus, we retain the $\mathcal{O}(|\mathbf{w}| + |\boldsymbol{\lambda}|)$ time and memory cost of Lorraine et al. (2019), where $|\cdot|$ denotes cardinality. The core loop to compute

the sum in (6) comes from an algorithm of Liao et al. (2018). Note that Algorithm 1 approximates $\frac{d\mathcal{L}_v}{d\lambda}$ retrospectively by considering only the last weight update rather than any future ones.

Unlike differentiation-through-optimisation (Domke, 2012), Algorithm 1 crucially estimates hypergradients without reference to old model parameters, thanks to the approximate-hypergradient construction of Lorraine et al. (2019) and (6). We thus do not store network weights at multiple time steps, so gradient-based HPO becomes possible on previously-intractable large-scale problems. In essence, we develop an approximation to online hypergradient descent (Baydin et al., 2018).

Optimiser hyperparameters generally do not affect the optimal weights, suggesting their hypergradients should be zero. However, in practice, \mathbf{w}^* is better reinterpreted as the *approximately* optimal weights obtained after a finite training episode. These certainly depend on the optimiser hyperparameters, which govern the convergence of \mathbf{w} , thus justifying our use of the bilevel framework.

We emphasise training is not reset after each hyperparameter update — we simply continue training from where we left off, using the new hyperparameters. Consequently, Algorithm 1 avoids the time cost of multiple training restarts. While our locally greedy hyperparameter updates threaten a short-horizon bias (Wu et al., 2018), we still realise practical improvements in our experiments.

2.5 REINTERPRETATION OF ITERATIVE OPTIMISATION

Originally, we stated the IFT (3) in terms of minima of \mathcal{L}_T (zeros of $\frac{\partial \mathcal{L}_T}{\partial \mathbf{w}}$), and substituting $\mathbf{u}_{\text{SGD}} = \eta \frac{\partial \mathcal{L}_T}{\partial \mathbf{w}}$ into (7) recovers this form of (3). However, in general, (7) recovers the Theorem for zeros of \mathbf{u} , which are not necessarily minima of the training loss. Despite this, our development can be compared to Lorraine et al. (2019) by expressing \mathbf{u} as the derivative of an augmented ‘pseudo-loss’ function. Consider again the simple SGD update \mathbf{u}_{SGD} , which provides the weight update rule $\mathbf{w}_i = \mathbf{w}_{i-1} - \eta \frac{\partial \mathcal{L}_T}{\partial \mathbf{w}}$. By trivially defining a pseudo-loss $\bar{\mathcal{L}} = \eta \mathcal{L}_T$, we may absorb η into a loss-like derivative, yielding $\mathbf{w}_i = \mathbf{w}_{i-1} - \frac{\partial \bar{\mathcal{L}}}{\partial \mathbf{w}}$. More generally, we may write $\bar{\mathcal{L}} = \int \mathbf{u}(\lambda, \mathbf{w}) d\mathbf{w}$.

Expressing the update in this form suggests a reinterpretation of the role of optimiser hyperparameters. Conventionally, our visualisation of gradient descent has the learning rate control the size of steps over some undulating landscape. Instead, we propose fixing a unit step size, with the ‘learning rate’ scaling the landscape underneath. Similarly, we suppose a ‘momentum’ could, at every point, locally squash the loss surface in the negative-gradient direction and stretch it in the positive-gradient direction. In aggregate, these transformations straighten out optimisation trajectories and bring local optima closer to the current point. While more complex hyperparameters lack a clear visualisation in this framework, it nevertheless allows a broader class of hyperparameters to ‘directly alter the loss function’ instead of remaining completely independent, circumventing the problem with optimiser hyperparameters noted by Lorraine et al. (2019). Figure 2 illustrates this argument.

3 RELATED WORK

Kohavi & John (1995) first noted different problems respond optimally to different hyperparameters; Hutter et al. (2018, Chapter 1) summarise the resulting *hyperparameter optimisation* (HPO) field.

Black-box HPO treats the training process as atomic, selecting trial configurations by grid search (coarse or intractable at scale), random search (Bergstra & Bengio (2012); often more efficient) or population-based searches (mutating promising trials). Pure Bayesian Optimisation (Moćkus et al., 1978; Snoek et al., 2012) guides the search with a predictive model; many works seek to exploit its sample efficiency (e.g. Swersky et al. (2014a); Snoek et al. (2015); Wang et al. (2016); Kandasamy et al. (2017); Lévesque et al. (2017); Perrone et al. (2019)). However, these methods require each proposed configuration to be fully trained, incurring considerable computational expense. Other techniques infer information *during* a training run — from learning curves (Provost et al., 1999; Swersky et al., 2014b; Domhan et al., 2015; Chandrashekar & Lane, 2017; Klein et al., 2017), smaller surrogate problems (Petrak, 2000; van den Bosch, A. et al., 2004; Krueger et al., 2015; Sparks et al., 2015; Thornton et al., 2013; Sabharwal et al., 2016) or intelligent resource allocation (Jamieson & Talwalkar, 2016; Li et al., 2018; Falkner et al., 2018; Bertrand et al., 2017; Wang et al., 2018). Such techniques could be applied on top of our algorithm to improve performance.

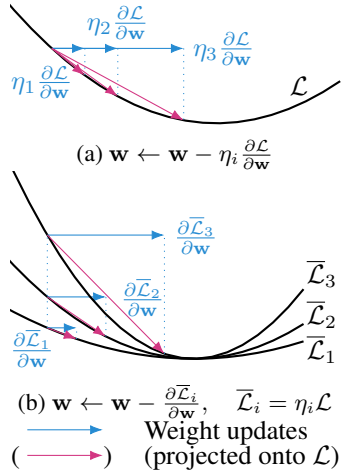


Figure 2: Reinterpreting the role of learning rate η over a loss function \mathcal{L} . (a) In the classical setting, η scales the gradient of some fixed \mathcal{L} . (b) In our setting, η scales \mathcal{L} to form a ‘pseudo-loss’ $\bar{\mathcal{L}}$, whose gradient is used as-is: our loss function has become dependent on η . The same weight updates are obtained in both (a) and (b).

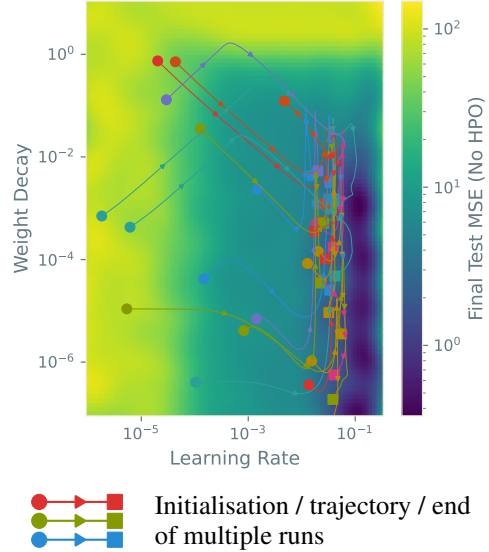


Figure 3: Sample hyperparameter trajectories from training UCI Energy under Our^{WD+LR} configuration. Background shading gives a non-HPO baseline with hyperparameters fixed at the corresponding initial point; these results are interpolated by a Gaussian process. Note the trajectories are generally attracted to the valley of high performance at learning rates around 10^{-1} and weight decays below 10^{-2} .

In HPO with nested *bilevel* optimisation, hyperparameters are optimised conditioned on optimal weights, enabling updates *during* training, with a separate validation set mitigating overfitting risk; this relates to meta-learning (Franceschi et al., 2018). Innovations include differentiable unrolled stochastic gradient descent (SGD) updates (Domke, 2012; Maclaurin et al., 2015; Baydin et al., 2018; Shaban et al., 2019; Majumder et al., 2019), conjugate gradients or hypernetworks (Lorraine & Duvenaud, 2018; Lorraine et al., 2019; MacKay et al., 2019; Fu et al., 2017), solving one level while penalising suboptimality of the other (Mehra & Hamm, 2020), and deploying Cauchy’s implicit function theorem (Larsen et al., 1996; Bengio, 2000; Luketina et al., 2016; Lorraine et al., 2019). Donini et al. (2020) extrapolate training to optimise arbitrary learning rate schedules, extending earlier work on gradient computation (Franceschi et al., 2017), but do not immediately accommodate other hyperparameters. While non-smooth procedures exist (Lopez-Ramos & Beferull-Lozano, 2020), most methods focus on smooth hyperparameters which augment the loss function (e.g. weight regularisation) and work with the augmented loss directly. Consequently, they cannot handle optimiser hyperparameters not represented in the loss function (e.g. learning rates and momentum factors; Lorraine et al. (2019)). Many of these methods compute hyperparameter updates locally (not over the entire training process), which may induce short-horizon bias (Wu et al., 2018), causing myopic convergence to local optima.

Modern developments include theoretical reformulations of bilevel optimisation to improve performance (Liu et al., 2020; Li et al., 2020), optimising distinct hyperparameters for each model parameter (Lorraine et al., 2019; Jie et al., 2020), and computing forward-mode hypergradient averages using more exact techniques than we do (Micaelli & Storkey, 2020). Although these approaches increase computational efficiency and the range of tunable parameters, achieving both benefits at once remains challenging. Our algorithm accommodates a diverse range of differentiable hyperparameters, but retains the efficiency of existing approaches (specifically Lorraine et al. (2019)).

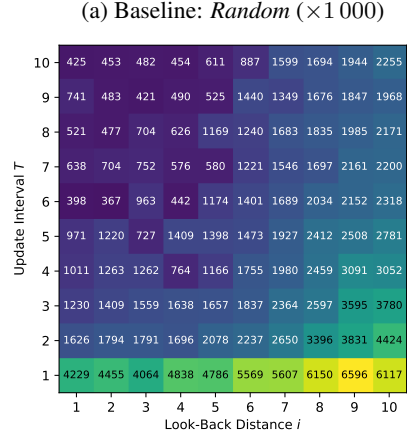
Algorithm 1
Scalable One-Pass Optimisation of High-Dimensional Weight-Update Hyperparameters by Implicit Differentiation

```

while training continues do
  for  $t \leftarrow 1$  to  $T$  do  $\triangleright T$  steps of weight updates
     $\mathbf{w} \leftarrow \mathbf{w} - \mathbf{u}(\boldsymbol{\lambda}, \mathbf{w})$ 
  end for
   $\mathbf{p} = \mathbf{v} = \left[ \frac{\partial \mathcal{L}_V}{\partial \mathbf{w}} \right]_{\boldsymbol{\lambda}, \mathbf{w}}$   $\triangleright$  Initialise accumulators
  for  $j \leftarrow 1$  to  $i$  do  $\triangleright$  Accumulate first summand in (6)
     $\mathbf{v} \leftarrow \mathbf{v} - \text{grad}(\mathbf{u}(\boldsymbol{\lambda}, \mathbf{w}), \mathbf{w}, \text{grad\_outputs} = \mathbf{v})$ 
     $\mathbf{p} \leftarrow \mathbf{p} + \mathbf{v}$ 
  end for  $\triangleright$  Now  $\mathbf{p} \approx \left[ \frac{\partial \mathcal{L}_V}{\partial \mathbf{w}} \left( \frac{\partial \mathbf{u}}{\partial \mathbf{w}} \right)^{-1} \right]_{\boldsymbol{\lambda}, \mathbf{w}}$ 
   $\mathbf{g}_{\text{indirect}} = -\text{grad}(\mathbf{u}(\boldsymbol{\lambda}, \mathbf{w}), \boldsymbol{\lambda}, \text{grad\_outputs} = \mathbf{p})$ 
   $\triangleright$  Now  $\mathbf{g}_{\text{indirect}} \approx - \left[ \frac{\partial \mathcal{L}_V}{\partial \mathbf{w}} \left( \frac{\partial \mathbf{u}}{\partial \mathbf{w}} \right)^{-1} \frac{\partial \mathbf{u}}{\partial \boldsymbol{\lambda}} \right]_{\boldsymbol{\lambda}, \mathbf{w}}$ 
   $\boldsymbol{\lambda} \leftarrow \boldsymbol{\lambda} - \kappa \left( \left[ \frac{\partial \mathcal{L}_V}{\partial \boldsymbol{\lambda}} \right]_{\boldsymbol{\lambda}, \mathbf{w}} + \mathbf{g}_{\text{indirect}} \right)$ 
   $\triangleright$  For some meta-learning rate  $\kappa$ 
end while

```

10812



(b) Our approach: *Ours*^{WD+LR+M} ($\times 1000$)

Figure 4: Left: Pseudocode for our method. Right: Median final test loss on UCI Energy after 400 hyperparameter updates from random initialisations, for various update intervals T and look-back distances i of (a) no hyper-parameter tuning, *Random*, and (b) our proposed method, *Ours*^{WD+LR+M}.

4 EXPERIMENTS

We now empirically evaluate our approach, using the hardware and software detailed in Appendix A.1. Our code is available at <https://github.com/rmclarke/OptimisingWeightUpdateHyperparameters>.

Throughout, we train models using SGD with weight decay and momentum. We uniformly sample initial learning rates, weight decays and momenta, using logarithmic and sigmoidal transforms (see Appendix B.3), applying each initialisation in the following eight settings:

- Random** No HPO; hyperparameters held constant at their initial values, as in random search.
- Random (\times LR)** *Random* with an extra hyperparameter increasing or decreasing the learning rate by multiplication after each update step.
- Random (3-batched)** *Random* reprocessed to retain only the best result of every three runs. Allows *Random* to exceed our methods’ computational budgets; imitates population training.
- Lorraine** Lorraine et al. (2019)’s method optimising weight decay; other hyperparameters constant.
- Baydin** Baydin et al. (2018)’s method optimising learning rates only; other hyperparameters constant.
- Ours^{WD+LR}** Algorithm 1 updating weight decay and learning rate; other hyperparameters constant.
- Ours^{WD+LR+M}** Optimising all hyperparameters (adding momentum to *Ours*^{WD+LR})
- Ours^{WD+HDLR+M}** *Ours*^{WD+LR+M} with independent learning rates for each model parameter
- Diff-through-Opt** Optimising all hyperparameters using exact hypergradients (Domke, 2012)

Any unoptimised hyperparameters are fixed at their random initial values. Ideally, we seek resilience to poor initialisations, which realistically arise in unguided hyperparameter selection. Hyperparameters are tuned on the validation set; this is combined with the training set for our *Random* settings, so each algorithm observes the same data. We use the UCI dataset split sizes of Gal & Ghahramani (2016) and standard 60%/20%/20% splits for training/validation/test datasets elsewhere, updating hyperparameters every $T = 10$ batches with look-back distance $i = 5$ steps.

Numerical data is normalised to zero-mean, unit-variance. For efficiency, the computational graph is detached after each hyperparameter update, so we never differentiate through hyperparameter updates — essentially, back-propagation and momentum histories are truncated. Our approximate hypergradient is passed to Adam (Kingma & Ba, 2015) with meta-learning rate $\kappa = 0.05$ and default $\beta_1 = 0.9, \beta_2 = 0.999$. While these *meta-hyperparameters* are not tuned, previous work indicates

Table 1: Final test MSEs after training UCI datasets for 4 000 full-batch epochs from each of 200 random hyperparameter initialisations, showing best and bootstrapped average runs. Uncertainties are standard errors; bold values lie in the error bars of the best algorithm.

Method	UCI Energy			UCI Kin8nm ($\times 1\,000$)			UCI Power		
	Mean	Median	Best	Mean	Median	Best	Mean	Median	Best
Random	21 ± 2	7.8 ± 0.4	0.120	38 ± 2	33 ± 3	6.44	67 ± 6	21 ± 2	15.4
Random ($\times LR$)	31 ± 2	13 ± 3	0.133	47 ± 2	45 ± 5	6.43	105 ± 8	35 ± 7	15.9
Random (3-batched)	4.5 ± 0.6	4 ± 2	0.141	18 ± 2	13 ± 1	6.72	19 ± 2	17.1 ± 0.2	15.5
Lorraine	22 ± 2	8.2 ± 0.5	0.161	38 ± 2	34 ± 3	6.39	67 ± 6	21 ± 1	16.4
Baydin	5.5 ± 0.2	6.70 ± 0.06	0.103	24.5 ± 0.8	27 ± 1	6.52	17.82 ± 0.07	17.93 ± 0.09	15.1
Ours ^{WD+LR}	2.5 ± 0.1	2.2 ± 0.2	0.147	10 ± 1	7.6 ± 0.1	6.44	17.33 ± 0.01	17.27 ± 0.01	15.5
Ours ^{WD+LR+M}	1.28 ± 0.08	0.9 ± 0.2	0.139	10 ± 1	6.95 ± 0.08	5.92	17.4 ± 0.2	17.231 ± 0.003	16.0
Ours ^{WD+HDLR+M}	1.9 ± 0.2	1.2 ± 0.3	0.165	16 ± 4	8.1 ± 0.1	6.29	18 ± 1	16.76 ± 0.04	16.0
Diff-through-Opt	1.10 ± 0.09	0.48 ± 0.09	0.123	8.0 ± 0.2	7.17 ± 0.06	6.09	17.17 ± 0.02	17.193 ± 0.005	15.3

performance is progressively less sensitive to higher-order hyperparameters (Franceschi et al., 2017; 2018; Majumder et al., 2019). As some settings habitually chose unstable high learning rates, we clip these to $[10^{-10}, 1]$ throughout.

UCI Energy: Proof of Concept First, we broadly illustrate Algorithm 1 on UCI Energy, using a one-layer multi-layer perceptron (MLP) with 50 hidden units and ReLU (Glorot et al., 2011) activation functions, trained under *Ours*^{WD+LR} for 4 000 full-batch epochs without learning rate clipping (see Appendix B.1 for details). Figure 3 shows the evolution of learning rate and weight decay from a variety of initialisations, overlaid on the performance obtained when all hyperparameters are kept fixed during training. Notice the trajectories are attracted towards the region of lowest test loss, indicating our algorithm is capable of useful learning rate and weight decay adjustment.

4.1 UCI DATASETS: ESTABLISHING ROBUSTNESS

Next, we consider the same 50-hidden-unit MLP applied to eight standard UCI datasets (Boston Housing, Concrete, Energy, Kin8nm, Naval, Power, Wine, Yacht) in a fashion analogous to Gal & Ghahramani (2016) (we do not consider dropout or Bayesian formulations). We train 200 hyperparameter initialisations for 4 000 full-batch epochs. Table 1 shows results for three datasets, with complete loss evolution and distribution plots in Appendix B.4. Some extreme hyperparameters caused numerical instability and NaN final losses, which our averages ignore. NaN results are not problematic: they indicate extremely poor initialisations, which should be easier for the user to rectify than merely mediocre hyperparameters. Error bars are based on 1 000 sets of bootstrap samples.

Given the sparse distribution of strong hyperparameter initialitions, random sampling unsurprisingly achieves generally poor averages. *Random* ($\times LR$) applies a learning rate multiplier, uniformly chosen in $[0.995, 1.001]$; these limits allow extreme initial learning rates to revert to more typical values after 4 000 multiplications. This setting’s poor performance shows naïve learning rate schedules cannot match our algorithms’ average improvements. A stronger baseline is *Random* (3-batched), which harshly simulates the greater computational cost of our methods by retaining only the best of every three *Random* trials (according to validation loss). This setting comes close to, but cannot robustly beat, our methods — a claim reinforced by final test loss distributions (Figure 9, Appendix B.4).

Lorraine et al. (2019)’s algorithm is surprisingly indistinguishable from *Random* in our trials, though it must account for three random hyperparameters while varying only one (the weight decay). We surmise that learning rates and momenta are more important hyperparameters to select, and poor choices cannot be overcome by intelligent use of weight decay. Baydin et al. (2018)’s algorithm, however, broadly matches the performance of *Random* (3-batched), indicating successful intervention in its sole optimisable hyperparameter (learning rate). Variance is also much lower than the preceding algorithms, suggesting greater stability. That said, despite concentrating on a more important hyperparameter, *Baydin* still suffers from being unable to control every hyperparameter.

Our scalar algorithms (*Ours*^{WD+LR} and *Ours*^{WD+LR+M}) appear generally more robust to these initialisations, with average losses beating *Random*, *Lorraine* and *Baydin*. Figures 8 and 9 (Appendix B.4) clearly distinguish these algorithms from the preceding: we achieve performant results over a wider space of initial hyperparameters. Given it considers more hyperparameters, *Ours*^{WD+LR+M} predictably outperforms *Ours*^{WD+LR}, although sometimes a slightly higher variance in the former obscures this

difference. Unlike pure HPO, the non-*Random* algorithms in Table 1 vary hyperparameters *during training*, combining aspects of HPO and schedule learning. They are thus more flexible than conventional, static-hyperparameter techniques, even in high dimensions (Lorraine et al., 2019).

Diff-through-Opt exactly differentiates the current loss with respect to the hyperparameters, over the same $i = 5$ look-back window and $T = 10$ update interval. As an exact version of *Ours*^{WD+LR+M} (though subject to the same short-horizon bias), it unsurprisingly outperforms the other algorithms (Figures 8 and 9, Appendix B.4). However, our scalar methods’ proximity to this exact baseline is reassuring given our much-reduced memory requirements and generally comparable error bars. In these experiments, lengthening *Diff-through-Opt*’s look-back horizon to all 4 000 training steps, and repeating those steps for 30 hyperparameter updates, did not improve its performance (Appendix B.7).

Ours^{WD+HDLR+M} theoretically mitigates short-horizon bias (Wu et al., 2018) by adapting appropriately to high- and low-curvature directions. Surprisingly, however, performance is often uncompetitive with scalar methods — training often diverges, causing large and wildly-varying final losses, which obscure very promising clusters of low-loss runs. In many of these runs, a subset of learning rates become large — presumably those for low-curvature directions. Large scalar learning rates are widely understood to yield high-variance results; it appears a similar phenomenon affects our high-dimensional algorithm. This punctuates a trend in our results: optimising more hyperparameters can lead to better solutions, but also provides more scope for divergent behaviour — possibly because we adapt to optimisation dynamics which suddenly change. We speculate learning rate regularisation would be beneficial, but leave investigation of high-dimensional dynamics to future work.

4.2 LARGE-SCALE DATASETS: PRACTICAL SCALABILITY

Fashion-MNIST: HPO in Multi-Layer Perceptrons We train the same single 50-unit hidden layer MLP on 10 epochs of Fashion-MNIST (Xiao et al., 2017), using 50-sample batches. Table 2 and Figure 12a (Appendix B.6) show average test set cross-entropies over 100 initialisations. Clearly-outlying final losses (above 10^3) are set to NaN to stop them dominating our error bars.

Echoing Section 4.1, for arbitrary hyperparameter initialisations, our methods generally converge more robustly to lower losses, even when (as in Figure 12a, Appendix B.6) NaN solutions are included in our statistics. Importantly, we see mini-batches provide sufficient gradient information for our HPO task. *Diff-through-Opt*’s failure to beat our methods is surprising; we suppose noisy approximate gradients may regularise our algorithms, preventing them seeking the short-horizon optimum so directly, thus mitigating short-horizon bias (see our sensitivity study in Section 4.3). *Diff-through-Opt* with long look-back horizons does not improve performance for equal computation (Appendix B.7). Finally, median and best loss evolution plots are shown in Figures 5b and 5c, the latter including results for a Bayesian Optimisation baseline. For more details, see Appendices B.5 and B.6.

Penn Treebank: HPO in Recurrent Networks Now, we draw inspiration from Lorraine et al. (2019)’s large-scale trials: a 2-layer, 650-unit LSTM (Hochreiter & Schmidhuber, 1997) with learnable embedding, trained on the standard Penn Treebank-3-subset benchmark dataset (Marcus et al., 1999) for 72 epochs. Lorraine et al.’s algorithm performed better without dropout, which we omit. To focus our study, we also omit activation regularisation and predefined learning rate schedules, though we retain training gradient clipping to a Euclidean norm of 0.25. Training considers

Table 2: Final test *cross-entropy (\dagger perplexity) on larger datasets. Bold values are the lowest in class.

Method	Fashion-MNIST*			Penn Treebank \dagger			CIFAR-10*		
	Mean	Median	Best	Mean	Median	Best	Mean	Median	Best
Random	0.85 \pm 0.07	0.51 \pm 0.05	0.334	4700 \pm 600	3000 \pm 3000	170	1.90 \pm 0.05	1.9 \pm 0.1	0.823
Random (\times LR)	1.62 \pm 0.08	2.0 \pm 0.2	0.446	7000 \pm 600	9400 \pm 700	138	20 \pm 20	1.7 \pm 0.1	0.798
Random (3-batched)	0.8 \pm 0.1	0.5 \pm 0.1	0.351	470 \pm 40	470 \pm 80	170	1.62 \pm 0.07	1.55 \pm 0.08	0.834
Lorraine	0.87 \pm 0.07	0.52 \pm 0.05	0.343	4700 \pm 600	3000 \pm 3000	170	1.70 \pm 0.06	1.6 \pm 0.1	0.727
Baydin	0.49 \pm 0.07	0.410 \pm 0.002	0.340	4200 \pm 600	1000 \pm 2000	147	1.55 \pm 0.04	1.5 \pm 0.1	0.762
Ours ^{WD+LR}	0.375 \pm 0.002	0.375 \pm 0.003	0.336	350 \pm 10	360 \pm 30	126	1.33 \pm 0.05	1.19 \pm 0.02	0.681
Ours ^{WD+LR+M}	0.374 \pm 0.002	0.373 \pm 0.003	0.336	290 \pm 50	220 \pm 20	103	1.23 \pm 0.05	1.17 \pm 0.02	0.631
Ours ^{WD+HDLR+M}	0.402 \pm 0.004	0.389 \pm 0.003	0.358	1300 \pm 900	300 \pm 600	190	1.59 \pm 0.07	1.6 \pm 0.1	0.735
Diff-through-Opt	0.388 \pm 0.001	0.387 \pm 0.002	0.359	300 \pm 10	280 \pm 20	114	1.196 \pm 0.008	1.202 \pm 0.006	0.941

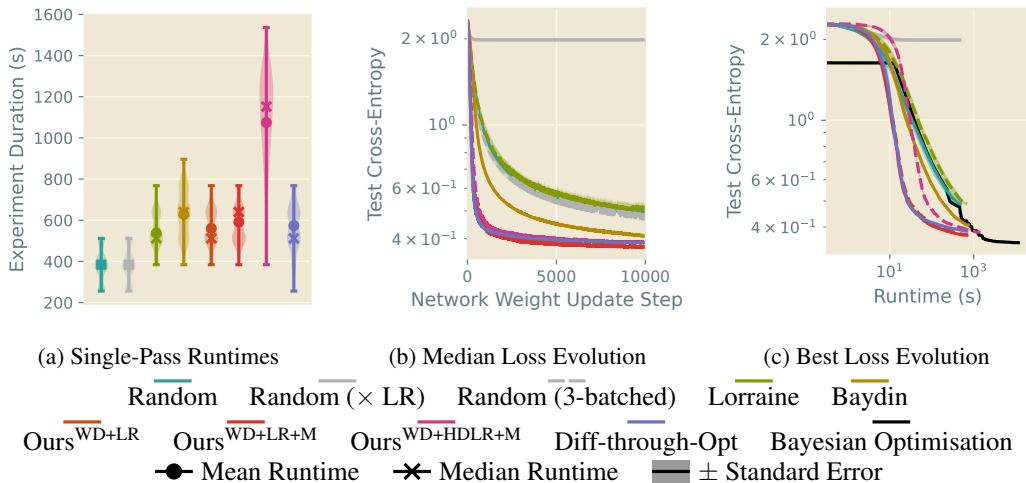


Figure 5: Illustrations of training a one-layer 50-unit MLP on Fashion-MNIST over 100 random hyperparameter initialisations. We include a *Bayesian Optimisation* baseline from Appendix B.5 and loss evolution plots from Appendix B.6.

length-70 subsequences of 40 parallel sequences, using 50 random hyperparameter initialisations. Again, clearly outlying final perplexities (above 10^5) are set to NaN.

Table 2 and Figure 12b (Appendix B.6) show final test perplexities. They reflect our intuition that adjusting progressively more hyperparameters reduces average test losses, continuing the trend we have seen thus far. Highly bimodal final loss distributions for some algorithms cause wide bootstrap-sampled error bars. Learning rate adjustments show particular gains: $Ours^{WD+LR}$ and $Ours^{WD+LR+M}$ perform well in less-optimal configurations. NaN runs — previously argued to be unproblematic — cause the largest performance differences between our methods (Figure 12b, Appendix B.6).

CIFAR-10: HPO in Convolutional Networks Finally, to demonstrate scalability, we train a ResNet-18 (He et al., 2016) on CIFAR-10 (Krizhevsky, 2009) for 72 epochs. We use the vanilla normalised dataset (since unbiased data augmentation over both training and validation datasets exhausts our GPU memory) and optimise hyperparameters as before, using 100-image batches.

Table 2 and Figure 12c (Appendix B.6) show our results. Our gains are now more marginal, with this setting apparently robust to its initialisation, though the general ranking of algorithms remains similar, and we retain useful improvements over our baselines. However, our best final accuracies fall short of state-of-the-art, suggesting a more intricate and clever setting may yield further performance gains.

4.3 MISCELLANEOUS STUDIES

Experiment Runtimes For our larger-scale experiments, we illustrate comparative runtimes in Figure 14 (Appendix B.6.1, where they are discussed in detail). Note from our Fashion-MNIST sample (Figure 5a) that all HPO algorithms except $Ours^{WD+HDLR+M}$ have computational cost similar to naively training two fixed hyperparameter initialisations, despite achieving substantial HPO effect. This compares extremely favourably to HPO methods relying on repeated retraining.

UCI Energy: Sensitivity Study Finally, we consider a range of update intervals T and look-back distances i on UCI Energy, performing 400 hyperparameter updates from 100 random initialisations on each, using $Ours^{WD+LR+M}$. We plot the median final test losses for each choice of T and i to the right of Figure 4, and also the median performance with no HPO (*Random*), which we outperform in every case. Performance generally improves with larger T — likely because the total number of weight updates increases with T , since the number of hyperparameter updates is fixed at 400. Performance also improves with smaller i . While a larger i gives more terms in our approximating series (6), these extra terms become more and more biased: they are evaluated at the current weight

values instead of at the progressively more different past weight values. We theorise a smaller i avoids some of this bias, improving performance. More details are given in Appendix B.2.

5 CONCLUSION AND FUTURE WORK

We have presented an algorithm for optimising continuous hyperparameters, specifically those appearing in a differentiable weight update, including optimiser hyperparameters. Our method requires only a single training pass, has a motivating true-hypergradient convergence argument, and demonstrates practical benefits at a range of experimental scales without greatly sacrificing training time. We also tackle traditionally-intractable per-parameter learning rate optimisation on non-trivial datasets. However, this setting surprisingly underperformed its scalar counterpart; further work is necessary to understand this result.

As future work, our myopic approach could be extended to longer horizons by incorporating the principles of recent work by Micaelli & Storkey (2020), which presents a promising research direction. We also depend inconveniently on meta-hyperparameters, which are not substantially tuned. Ultimately, we desire systems which are completely independent of human configuration, thus motivating investigations into the removal of these settings.

SOCIETAL IMPACT / ETHICS STATEMENT

Our work fits into the broad subfield of automatic machine learning (AutoML), which aims to use automation to strip away the tedious work that is necessary to implement practical ML systems. Our method focuses on automating the oft-labelled ‘black art’ of optimising hyperparameters. This contributes towards the democratisation of ML techniques, which we hope will improve accessibility to non-experts.

However, our method also has some associated risks. For one, developers of unethical machine learning applications (e.g. for mass surveillance, identity theft or automated weaponry) may use our techniques to improve their systems’ performance. The heavily metric-dominated nature of our field creates additional concerns — for instance, end-users of our method may not appreciate that optimising naïvely for training and validation loss alone may result in dangerously poorly-trained or unethical models if the chosen metric, developer’s intentions and moral good do not align.

More broadly, users may rely excessively on HPO techniques to optimise their models’ performance, which can lead to poor results and inaccurate comparisons if the HPO strategy is imperfect. Further, reducing the need to consider hyperparameter tuning abstracts away an important component of how machine learning methods work in practice. Knowledge of this component may then become less accessible, inhibiting understanding and future research insights from the wider community.

Our datasets are drawn from standard benchmarks, and thus should not introduce new societal risks. Similarly, our work aims to decrease the computational burden of HPO, which should mitigate the environmental impact of ML training — an ever more important goal in our increasingly environmentally-conscious society.

REPRODUCIBILITY STATEMENT

All datasets we use are publicly available; for the Penn Treebank dataset, we provide a link in Table 4 (Appendix A.2). What little data processing we perform is fully explained in the corresponding subsection of Section 4.

Our mathematical arguments are presented fully and with disclosure of all assumptions in Section C.

Source code for all our experiments is provided to reviewers, and is made available on GitHub (<https://github.com/rmclarke/OptimisingWeightUpdateHyperparameters>). This source code contains a complete description of our experimental environment, configuration files and instructions on the reproduction of our experiments.

ACKNOWLEDGEMENTS

We acknowledge computation provided by the Cambridge Service for Data Driven Discovery (CSD3) operated by the University of Cambridge Research Computing Service (www.csd3.cam.ac.uk), provided by Dell EMC and Intel using Tier-2 funding from the Engineering and Physical Sciences Research Council (capital grant EP/P020259/1), and DiRAC funding from the Science and Technology Facilities Council (www.dirac.ac.uk).

We thank Austin Tripp for his feedback on drafts of this paper.

Ross Clarke acknowledges funding from the Engineering and Physical Sciences Research Council (project reference 2107369, grant EP/S515334/1).

REFERENCES

- Baydin, A. G., Cornish, R., Rubio, D. M., Schmidt, M., and Wood, F. Online Learning Rate Adaptation with Hypergradient Descent. *arXiv:1703.04782 [cs, stat]*, February 2018.
- Bengio, Y. Gradient-Based Optimization of Hyperparameters. *Neural Computation*, 12(8):1889–1900, August 2000.
- Bergstra, J. and Bengio, Y. Random Search for Hyper-Parameter Optimization. *Journal of Machine Learning Research*, 13(Feb):281–305, 2012.
- Bertrand, H., Ardon, R., Perrot, M., and Bloch, I. Hyperparameter Optimization of Deep Neural Networks: Combining Hyperband with Bayesian Model Selection. In *Conférence Sur l’Apprentissage Automatique*, pp. 5, 2017.
- Bouthillier, X. and Varoquaux, G. Survey of machine-learning experimental methods at NeurIPS2019 and ICLR2020. Research Report, Inria Saclay Ile de France, January 2020.
- Chandrashekar, A. and Lane, I. R. Speeding up Hyper-parameter Optimization by Extrapolation of Learning Curves Using Previous Builds. In Ceci, M., Hollmén, J., Todorovski, L., Vens, C., and Džeroski, S. (eds.), *Machine Learning and Knowledge Discovery in Databases*, Lecture Notes in Computer Science, pp. 477–492, Cham, 2017. Springer International Publishing.
- Domhan, T., Springenberg, J. T., and Hutter, F. Speeding Up Automatic Hyperparameter Optimization of Deep Neural Networks by Extrapolation of Learning Curves. In *Twenty-Fourth International Joint Conference on Artificial Intelligence*, June 2015.
- Domke, J. Generic Methods for Optimization-Based Modeling. In *Artificial Intelligence and Statistics*, pp. 318–326, March 2012.
- Donini, M., Franceschi, L., Frasconi, P., Pontil, M., and Majumder, O. MARTHE: Scheduling the Learning Rate Via Online Hypergradients. In *Twenty-Ninth International Joint Conference on Artificial Intelligence*, volume 3, pp. 2119–2125, July 2020.
- Falkner, S., Klein, A., and Hutter, F. BOHB: Robust and Efficient Hyperparameter Optimization at Scale. In *International Conference on Machine Learning*, pp. 1437–1446. PMLR, July 2018.
- Franceschi, L., Donini, M., Frasconi, P., and Pontil, M. Forward and Reverse Gradient-Based Hyperparameter Optimization. In *International Conference on Machine Learning*, pp. 1165–1173, July 2017.
- Franceschi, L., Frasconi, P., Salzo, S., Grazzi, R., and Pontil, M. Bilevel Programming for Hyperparameter Optimization and Meta-Learning. In *International Conference on Machine Learning*, pp. 1568–1577. PMLR, July 2018.
- Fu, J., Ng, R., Chen, D., Ilievski, I., Pal, C., and Chua, T.-S. Neural Optimizers with Hypergradients for Tuning Parameter-Wise Learning Rates. In *Automatic Machine Learning Workshop at ICML 2017*, pp. 8, Sydney, August 2017.
- Gal, Y. and Ghahramani, Z. Dropout as a Bayesian Approximation: Representing Model Uncertainty in Deep Learning. In *International Conference on Machine Learning*, pp. 1050–1059, June 2016.

- Glorot, X., Bordes, A., and Bengio, Y. Deep Sparse Rectifier Neural Networks. In *Proceedings of the Fourteenth International Conference on Artificial Intelligence and Statistics*, pp. 315–323, June 2011.
- Grefenstette, E., Amos, B., Yarats, D., Htut, P. M., Molchanov, A., Meier, F., Kiela, D., Cho, K., and Chintala, S. Generalized Inner Loop Meta-Learning. *arXiv:1910.01727 [cs, stat]*, October 2019.
- He, K., Zhang, X., Ren, S., and Sun, J. Deep Residual Learning for Image Recognition. In *2016 IEEE Conference on Computer Vision and Pattern Recognition (CVPR)*, pp. 770–778, June 2016.
- Hochreiter, S. and Schmidhuber, J. Long Short-Term Memory. *Neural Computation*, 9(8):1735–1780, November 1997.
- Hutter, F., Kotthoff, L., and Vanschoren, J. (eds.). *Automated Machine Learning: Methods, Systems, Challenges*. Springer, 2018.
- Jamieson, K. and Talwalkar, A. Non-stochastic Best Arm Identification and Hyperparameter Optimization. In *Proceedings of the 19th International Conference on Artificial Intelligence and Statistics*, pp. 240–248, May 2016.
- Jie, R., Gao, J., Vasnev, A., and Tran, M.-N. Adaptive Multi-level Hyper-gradient Descent. *arXiv:2008.07277 [cs]*, August 2020.
- Kandasamy, K., Dasarthy, G., Schneider, J., and Poczos, B. Multi-fidelity Bayesian Optimisation with Continuous Approximations. *arXiv:1703.06240 [stat]*, March 2017.
- Kingma, D. P. and Ba, J. Adam: A Method for Stochastic Optimization. In *arXiv:1412.6980 [Cs]*, San Diego, CA, USA, May 2015.
- Klein, A., Falkner, S., Springenberg, J. T., and Hutter, F. Learning Curve Prediction with Bayesian Neural Networks. In *5th International Conference on Learning Representations*, 2017.
- Kohavi, R. and John, G. H. Automatic Parameter Selection by Minimizing Estimated Error. In Prieditis, A. and Russell, S. (eds.), *Machine Learning Proceedings 1995*, pp. 304–312. Morgan Kaufmann, San Francisco (CA), January 1995.
- Krizhevsky, A. *Learning Multiple Layers of Features from Tiny Images*. MSc Thesis, University of Toronto, April 2009.
- Krueger, T., Panknin, D., and Braun, M. Fast Cross-Validation via Sequential Testing. *Journal of Machine Learning Research*, 16(33):1103–1155, 2015.
- Larsen, J., Hansen, L., Svarer, C., and Ohlsson, M. Design and regularization of neural networks: The optimal use of a validation set. In *Neural Networks for Signal Processing VI. Proceedings of the 1996 IEEE Signal Processing Society Workshop*, pp. 62–71, September 1996.
- Lévesque, J., Durand, A., Gagné, C., and Sabourin, R. Bayesian optimization for conditional hyperparameter spaces. In *2017 International Joint Conference on Neural Networks (IJCNN)*, pp. 286–293, May 2017.
- Li, J., Gu, B., and Huang, H. Improved Bilevel Model: Fast and Optimal Algorithm with Theoretical Guarantee. *arXiv:2009.00690 [cs, stat]*, September 2020.
- Li, L., Jamieson, K., DeSalvo, G., Rostamizadeh, A., and Talwalkar, A. Hyperband: A Novel Bandit-Based Approach to Hyperparameter Optimization. *arXiv:1603.06560 [cs, stat]*, June 2018.
- Liao, R., Xiong, Y., Fetaya, E., Zhang, L., Yoon, K., Pitkow, X., Urtasun, R., and Zemel, R. Reviving and Improving Recurrent Back-Propagation. In *International Conference on Machine Learning*, pp. 3082–3091. PMLR, July 2018.
- Liu, R., Mu, P., Yuan, X., Zeng, S., and Zhang, J. A Generic First-Order Algorithmic Framework for Bi-Level Programming Beyond Lower-Level Singleton. In *Proceedings of the International Conference on Machine Learning*. PMLR, 2020.

- Lopez-Ramos, L. M. and Beferull-Lozano, B. Online Hyperparameter Search Interleaved with Proximal Parameter Updates. *arXiv:2004.02769 [cs, eess, stat]*, April 2020.
- Lorraine, J. and Duvenaud, D. Stochastic Hyperparameter Optimization through Hypernetworks. *arXiv:1802.09419 [cs]*, March 2018.
- Lorraine, J., Vicol, P., and Duvenaud, D. Optimizing Millions of Hyperparameters by Implicit Differentiation. *arXiv:1911.02590 [cs, stat]*, November 2019.
- Luketina, J., Berglund, M., Greff, K., and Raiko, T. Scalable Gradient-Based Tuning of Continuous Regularization Hyperparameters. In *International Conference on Machine Learning*, pp. 2952–2960. PMLR, June 2016.
- MacKay, M., Vicol, P., Lorraine, J., Duvenaud, D., and Grosse, R. Self-Tuning Networks: Bilevel Optimization of Hyperparameters using Structured Best-Response Functions. *arXiv:1903.03088 [cs, stat]*, March 2019.
- Maclaurin, D., Duvenaud, D., and Adams, R. Gradient-based Hyperparameter Optimization through Reversible Learning. In *International Conference on Machine Learning*, pp. 2113–2122. PMLR, June 2015.
- Majumder, O., Donini, M., and Chaudhari, P. Learning the Learning Rate for Gradient Descent by Gradient Descent. In *6th AutoML Workshop at ICML 2019*, pp. 8, 2019.
- Marcus, M. P., Santorini, B., Marcinkiewicz, M. A., and Taylor, A. Treebank-3, 1999.
- Mehra, A. and Hamm, J. Penalty Method for Inversion-Free Deep Bilevel Optimization. *arXiv:1911.03432 [cs, math, stat]*, June 2020.
- Micaelli, P. and Storkey, A. Non-greedy Gradient-based Hyperparameter Optimization Over Long Horizons. *arXiv:2007.07869 [cs, stat]*, July 2020.
- Močkus, J., Tiešis, V., and Žilinskas, A. The Application of Bayesian Methods for Seeking the Extremum. *Towards Global Optimisation*, 2:117–129, 1978.
- Nogueira, F. Bayesian Optimization: Open source constrained global optimization tool for Python, 2014.
- Paszke, A., Gross, S., Massa, F., Lerer, A., Bradbury, J., Chanan, G., Killeen, T., Lin, Z., Gimelshein, N., Antiga, L., Desmaison, A., Kopf, A., Yang, E., DeVito, Z., Raison, M., Tejani, A., Chilamkurthy, S., Steiner, B., Fang, L., Bai, J., and Chintala, S. PyTorch: An Imperative Style, High-Performance Deep Learning Library. In *Advances in Neural Information Processing Systems 32 (NeurIPS 2019)*, pp. 12, Vancouver, Canada, 2019.
- Pearlmutter, B. A. Fast exact multiplication by the Hessian. *Neural Computation*, 6(1):147–160, January 1994.
- Pedregosa, F., Varoquaux, G., Gramfort, A., Michel, V., Thirion, B., Grisel, O., Blondel, M., Prettenhofer, P., Weiss, R., Dubourg, V., Vanderplas, J., Passos, A., Cournapeau, D., Brucher, M., Perrot, M., and Duchesnay, É. Scikit-learn: Machine Learning in Python. *Journal of Machine Learning Research*, 12(85):2825–2830, 2011.
- Perrone, V., Shen, H., Seeger, M., Archambeau, C., and Jenatton, R. Learning search spaces for Bayesian optimization: Another view of hyperparameter transfer learning. *arXiv:1909.12552 [cs, stat]*, September 2019.
- Petrak, J. Fast Subsampling Performance Estimates for Classification Algorithm Selection. Technical Report TR-2000-07, Austrian Research Institute for Artificial Intelligence, 2000.
- Provost, F., Jensen, D., and Oates, T. Efficient progressive sampling. In *Proceedings of the Fifth ACM SIGKDD International Conference on Knowledge Discovery and Data Mining, KDD '99*, pp. 23–32, San Diego, California, USA, August 1999. Association for Computing Machinery.

- Sabharwal, A., Samulowitz, H., and Tesauro, G. Selecting near-optimal learners via incremental data allocation. In *Proceedings of the Thirtieth AAAI Conference on Artificial Intelligence*, AAAI'16, pp. 2007–2015, Phoenix, Arizona, February 2016. AAAI Press.
- Shaban, A., Cheng, C.-A., Hatch, N., and Boots, B. Truncated Back-propagation for Bilevel Optimization. In *The 22nd International Conference on Artificial Intelligence and Statistics*, pp. 1723–1732, April 2019.
- Snoek, J., Larochelle, H., and Adams, R. P. Practical Bayesian Optimization of Machine Learning Algorithms. In Pereira, F., Burges, C. J. C., Bottou, L., and Weinberger, K. Q. (eds.), *Advances in Neural Information Processing Systems 25*, pp. 2951–2959. Curran Associates, Inc., 2012.
- Snoek, J., Rippel, O., Swersky, K., Kiros, R., Satish, N., Sundaram, N., Patwary, M., Prabhat, M., and Adams, R. Scalable Bayesian Optimization Using Deep Neural Networks. In *International Conference on Machine Learning*, pp. 2171–2180. PMLR, June 2015.
- Sparks, E. R., Talwalkar, A., Haas, D., Franklin, M. J., Jordan, M. I., and Kraska, T. Automating model search for large scale machine learning. In *Proceedings of the Sixth ACM Symposium on Cloud Computing*, SoCC '15, pp. 368–380, Kohala Coast, Hawaii, August 2015. Association for Computing Machinery.
- Swersky, K., Duvenaud, D., Snoek, J., Hutter, F., and Osborne, M. A. Raiders of the Lost Architecture: Kernels for Bayesian Optimization in Conditional Parameter Spaces. *arXiv:1409.4011 [stat]*, September 2014a.
- Swersky, K., Snoek, J., and Adams, R. P. Freeze-Thaw Bayesian Optimization. *arXiv:1406.3896 [cs, stat]*, June 2014b.
- Thornton, C., Hutter, F., Hoos, H. H., and Leyton-Brown, K. Auto-WEKA: Combined selection and hyperparameter optimization of classification algorithms. In *Proceedings of the 19th ACM SIGKDD International Conference on Knowledge Discovery and Data Mining*, KDD '13, pp. 847–855, Chicago, Illinois, USA, August 2013. Association for Computing Machinery.
- Turner, R., Eriksson, D., McCourt, M., Kiili, J., Laaksonen, E., Xu, Z., and Guyon, I. Bayesian Optimization is Superior to Random Search for Machine Learning Hyperparameter Tuning: Analysis of the Black-Box Optimization Challenge 2020. *arXiv:2104.10201 [cs, stat]*, August 2021.
- van den Bosch, A., Verbrugge, R., Taatgen, N., and Schomaker, L. Wrapped progressive sampling search for optimizing learning algorithm parameters. In *Proceedings of the Belgium-Netherlands Conference on Artificial Intelligence, BNAIC'04*, pp. 219–226, October 2004.
- Wang, J., Xu, J., and Wang, X. Combination of Hyperband and Bayesian Optimization for Hyperparameter Optimization in Deep Learning. *arXiv:1801.01596 [cs]*, January 2018.
- Wang, Z., Hutter, F., Zoghi, M., Matheson, D., and de Feitas, N. Bayesian Optimization in a Billion Dimensions via Random Embeddings. *Journal of Artificial Intelligence Research*, 55:361–387, February 2016.
- Williams, C. K. I. and Rasmussen, C. E. Gaussian Processes for Regression. In Touretzky, D. S., Mozer, M. C., and Hasselmo, M. E. (eds.), *Advances in Neural Information Processing Systems 8*, pp. 514–520. MIT Press, 1996.
- Wu, Y., Ren, M., Liao, R., and Grosse, R. B. Understanding Short-Horizon Bias in Stochastic Meta-Optimization. In *6th International Conference on Learning Representations*, Vancouver, BC, Canada, 2018. OpenReview.net.
- Xiao, H., Rasul, K., and Vollgraf, R. Fashion-MNIST: A Novel Image Dataset for Benchmarking Machine Learning Algorithms. *arXiv:1708.07747 [cs, stat]*, September 2017.

A NOTES

A.1 EXPERIMENTAL CONFIGURATION

Table 3: Hardware configurations used to run our experiments.

Type	CPU (Intel)	GPU (NVIDIA)
Consumer Desktop	Core i7-3930K	RTX 2080GTX
Local Cluster	Xeon E5-2680 Core i9-10900X	Tesla P100 RTX 2080GTX
Cambridge Service for Data Driven Discovery (CSD3)*	Xeon E5-2650	Tesla P100

* www.csd3.cam.ac.uk

Our experiments are variously performed on one of four sets of hardware, as detailed in Table 3. While system configurations varied between experiments, this does not impair comparability. All Penn Treebank and CIFAR-10 experiments were performed on the CSD3 Cluster; otherwise, all experiments comparing runtimes were performed on the Core i9 Local Cluster. We make use of GPU acceleration throughout, with the PyTorch (Paszke et al., 2019) and Higher (Grefenstette et al., 2019) libraries.

A.2 DATASET LICENCES

Table 4: Licences under which we use datasets in this work.

Dataset	Licence	Source
UCI Boston UCI Concrete UCI Energy UCI Kin8nm UCI Naval UCI Power UCI Wine UCI Yacht	Unknown; widely used	Gal & Ghahramani (2016, Github)
Fashion-MNIST	MIT	PyTorch via <code>torchvision</code>
Penn Treebank	Proprietary; fair use subset, widely used	*
CIFAR-10	No licence specified	PyTorch via <code>torchvision</code>

* <http://www.fit.vutbr.cz/~imikolov/rnnlm/simple-examples.tgz>

Our datasets are all standard in the ML literature. For completeness, we outline the licences under which they are used in Table 4.

B ADDITIONAL RESULTS

B.1 UCI ENERGY: PROOF OF CONCEPT

Our proof of concept graphic (Figure 3) is constructed using the same experimental configuration as Section 4.1, but without hyperparameter clipping of the learning rate, so our algorithm’s natural behaviour is displayed. Training 500 random initialisations of the model, weight decay and learning rate for 4 000 network weight update steps on *Random* (without any HPO) yields source data for the heatmap forming the background of Figure 3. The heatmap itself is the predictive mean of a Gaussian process (Williams & Rasmussen, 1996) using the sum of an RBF and white noise kernel. We fit the Gaussian process in log (input and output) space using the defaults of the Scikit-learn implementation (Pedregosa et al., 2011), which automatically select hyperparameters for the kernels. We then train a small number of additional initialisations using *Ours*^{WD+LR} and plot these trajectories. As always, the training set provides network weight updates, the validation set provides hyperparameter updates and

our results plot final performance on the test set. While we do not expect the optimal trajectory during training to coincide with gradients of our background heatmap, the latter provides useful context.

Generally, given our limited training budget, larger learning rates improve final performance up to a point, then cause instability if taken to extremes, and the movement of our trajectories reflects this. Many trajectories select large weight decay coefficients before doubling back on themselves to smaller weight decays — suggestive of our algorithm using the weight decay to avoid converging to specific minima. Trajectories generally converge to the valley of good test performance at a learning rate of around 10^{-1} and weight decay below 10^{-2} , further demonstrating appropriate behaviour. In short, we are able to make sensible and interpretable updates to the hyperparameters of this problem, which lends support to the applicability of our method.

B.2 UCI ENERGY: ADDITIONAL STUDIES

Our sensitivity studies are based on a similar experimental configuration to Section 4.1: for each choice of update interval T and look-back distance i , we generate 100 random initialisations of weight decay, learning rate and momentum. Each initialisation is trained for 400 hyperparameter steps, so increasing T permits more network weight updates; averaging over the 100 final test losses yields each result cell in Figure 6 and Figure 7. We do not perform any clipping of the learning rates, so as to allow the natural behaviour of each algorithm to be displayed. As in Section 4.1, we consider the *Ours*^{WD+LR+M} and *Diff-through-Opt* algorithms, optimising hyperparameters using Adam with hyper-learning rate $\kappa = 0.05$ and truncating gradient histories at the previous hyperparameter update.

B.2.1 SENSITIVITY OF UPDATE INTERVAL AND LOOK-BACK DISTANCE



(a) *Random* ($\times 1000$)

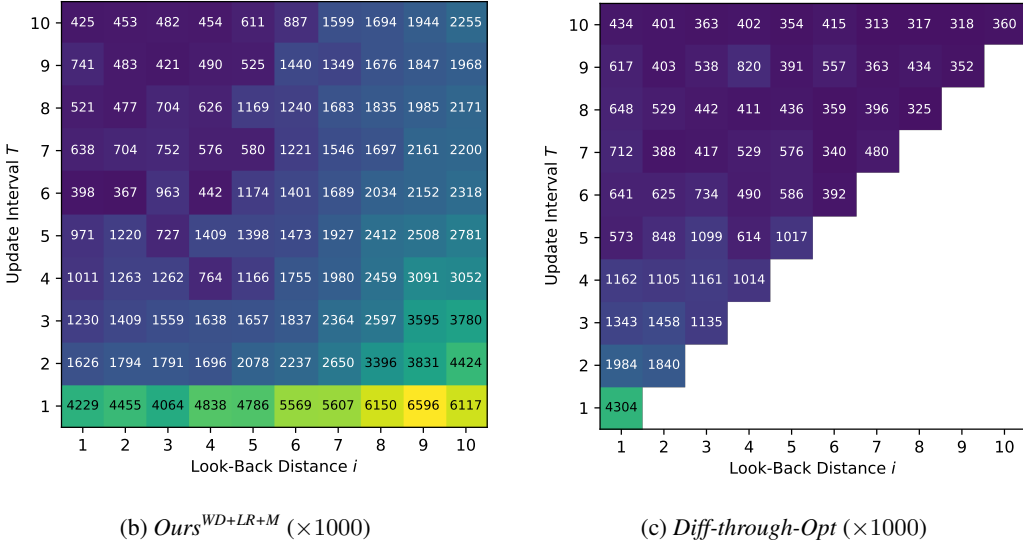


Figure 6: Median final test loss over 100 repetitions, after optimising UCI Energy for 400 hyperparameter update steps, from a variety of update intervals T and look-back distances i .

Figure 6 shows our final performance results in this setting: our algorithm’s strongest configurations (Figure 6b) compare favourably with results obtained using the exact hypergradients of *Diff-through-Opt* (Figure 6c). Noting that the conditions necessary to guarantee our algorithm’s convergence to the best-response derivative (specifically that the current network weights are optimal for the current

hyperparameters) are almost certainly not met in practice, it is unsurprising that *Diff-through-Opt* achieves greater performance. This difference is much smaller, however, than that between both HPO algorithms and the *Random* base case; given our substantial efficiency benefits over *Diff-through-Opt*, we make an acceptable compromise between accuracy and scalability. Further, these results justify our choice of $T = 10$ and $i = 5$ to match the setting of Lorraine et al. (2019). That said, recall these figures enforce consistency of number of hyperparameter updates, not of total computational expense; there remains a case for using large numbers of less precise hyperparameter updates (small T and i), which may promote faster convergence in practice.

B.2.2 ACCURACY OF HYPERGRADIENTS

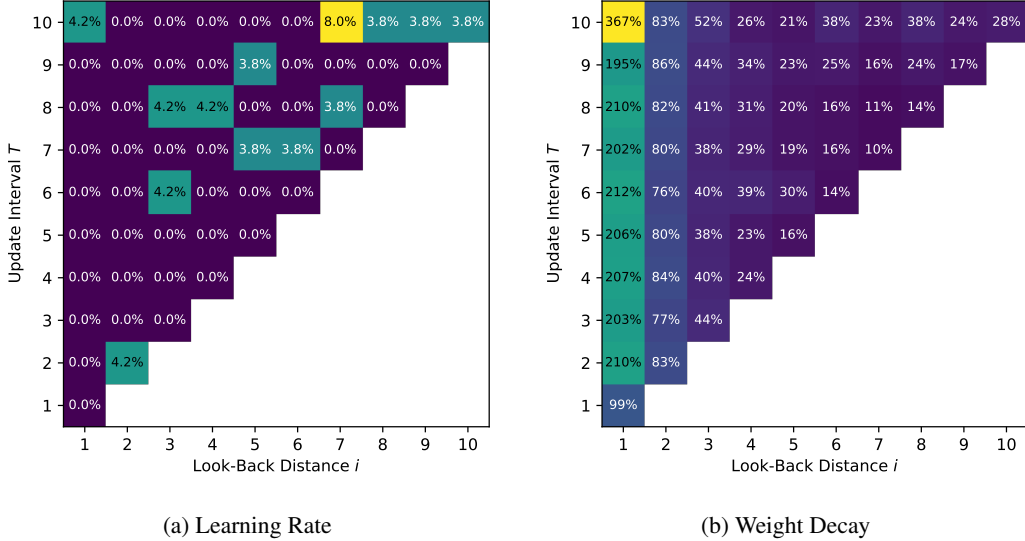


Figure 7: Mean absolute error in our approximate hypergradients, based on the first hyperparameter updates of 50 repetitions for each cell, using UCI Energy. We vary the update interval T and look-back distance i to investigate the sensitivity of the problem to these meta-hyperparameters. Hypergradients are shown separately for each hyperparameter.

We use this same experimental setting to evaluate the accuracy of our approximate hypergradients. Our approximate and exact settings are only guaranteed to be trying to compute the same hypergradient at the very first hyperparameter update, so we consider this time step only. Using those first hyperparameter updates from 50 random initialisations of hyperparameter and model, we compute the absolute error of the approximate hypergradient ($Ours^{WD+LR+M}$) as a percentage of the exact hypergradient (*Diff-through-Opt*), then plot the means of these errors in Figure 7.

Notice our learning rate hypergradients do not exhibit any particularly strong trends over the meta-hyperparameters we consider, but our approximate weight decay hypergradients seem to benefit from a shorter update interval and higher look-back distance. Some of the latter average proportional errors are large; a closer examination of the error distributions reveals these hypergradients have heavy tails at high errors. We hypothesise that the generally very small weight decay coefficients present more opportunity for numerical computational error than the generally larger learning rates, in which case hypergradients for different hyperparameters may have markedly different accuracies. However, our previous coarser studies suggest that, despite being approximate, our method does not suffer catastrophically from inaccurate hypergradients.

B.3 EXPERIMENT DETAILS

Table 5: Transformation and initialisation parameters used in our hyperparameter optimisation.

Hyperparameter	Initialisation Space	Initialisation Range		Optimisation Space	Natural Range	
		Min	Max		Min	Max
Learning Rate	Logarithmic	-6	-1	Logarithmic	1×10^{-6}	0.1
Weight Decay	Logarithmic	-7	-2	Logarithmic	1×10^{-7}	0.01
Momentum	Natural	0	1	Sigmoidal	0	1

Since the hyperparameters associated with SGD only take meaningful values on subsets of the real line, we apply gradient descent to transformed versions of the hyperparameters. For non-negative hyperparameters, such as learning rate and weight decay, we work with the base-10 logarithm of the actual value; for momentum, which lies in the unit interval $[0, 1]$, we work with the inverse-sigmoid of the actual value. These transformed search spaces mean a naïve implementation of gradient descent will not update hyperparameters to nonsensical values.

Our hyperparameter initialisations are drawn uniformly from a broad range, intended to be a superset of typical values to permit analysis of the realistic case where we have little intuition for the optimal choices. Thus, our hyperparameter ranges include typical values for a variety of applications, while giving each algorithm the opportunity to briefly stretch into more extreme values should these be useful on occasion. Where we have applied a logarithmic transformation to a hyperparameter (learning rate and weight decay), we draw samples uniformly in logarithmic space; where inverse-sigmoid transforms are used (momentum), we draw samples in natural space to ensure adequate exploration of values near 0 and 1. Table 5 summarises our initialisation and optimisation strategy.

B.4 UCI DATASETS

Results from all UCI datasets we considered are presented in Figures 8 and 9. These show many of the features already discussed in Section 4.1. We account for experimental runs ending in NaN losses by appropriately scaling the maximum value of the CDFs in Figure 9 to be less than 1.0. For each dataset, one random configuration is selected, and the resulting learning rate evolutions plotted in Figure 10. Note that UCI Naval generated a large number of NaN runs, which explains the apparent absence of certain algorithms from its graphs.

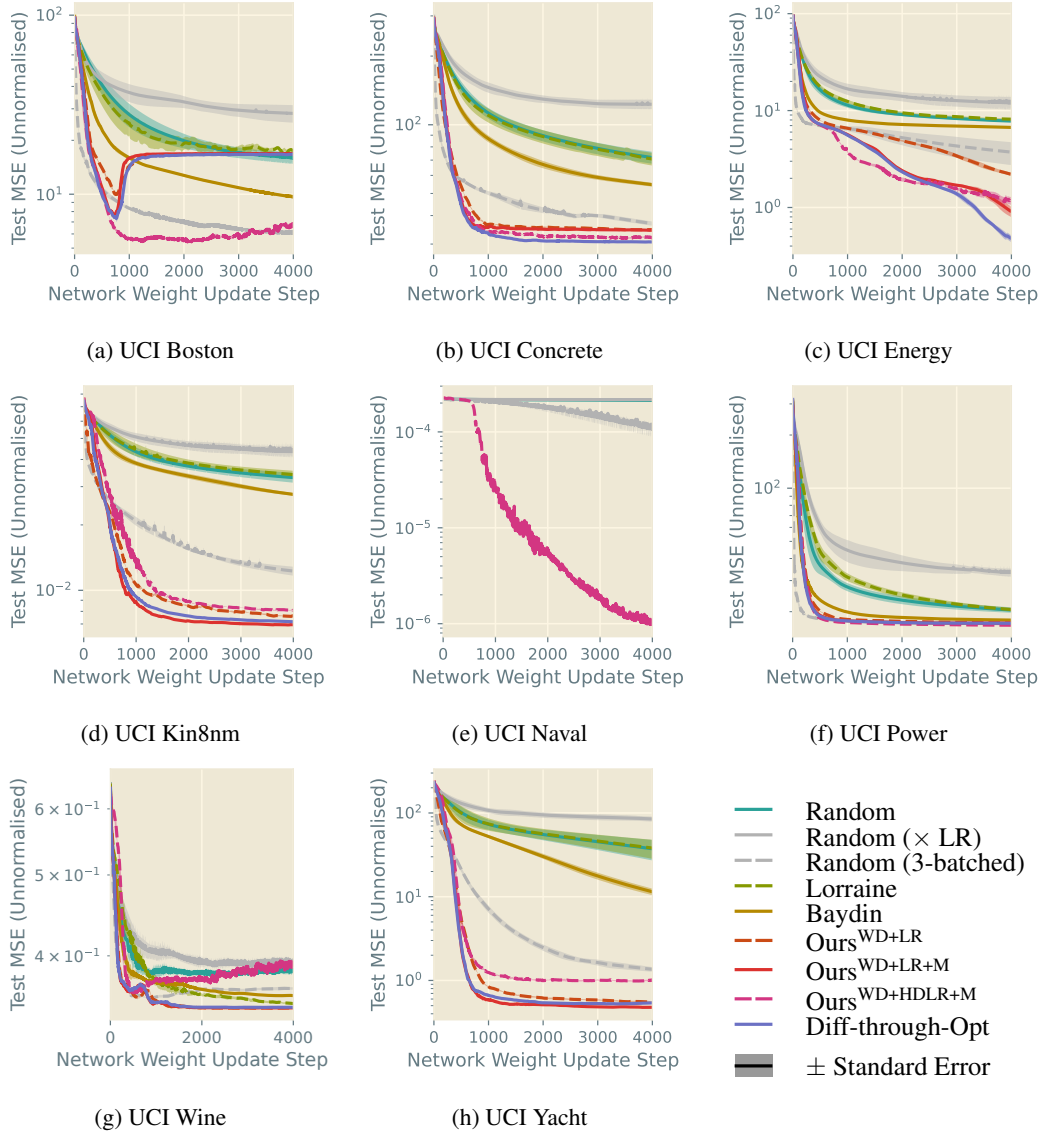


Figure 8: Evolution of test MSEs during training of UCI datasets for 4 000 full-batch epochs from each of 200 random initialisations of SGD learning rate, weight decay and momentum. We bootstrap sample our results to construct a median test MSE estimator at each update step and its standard error.

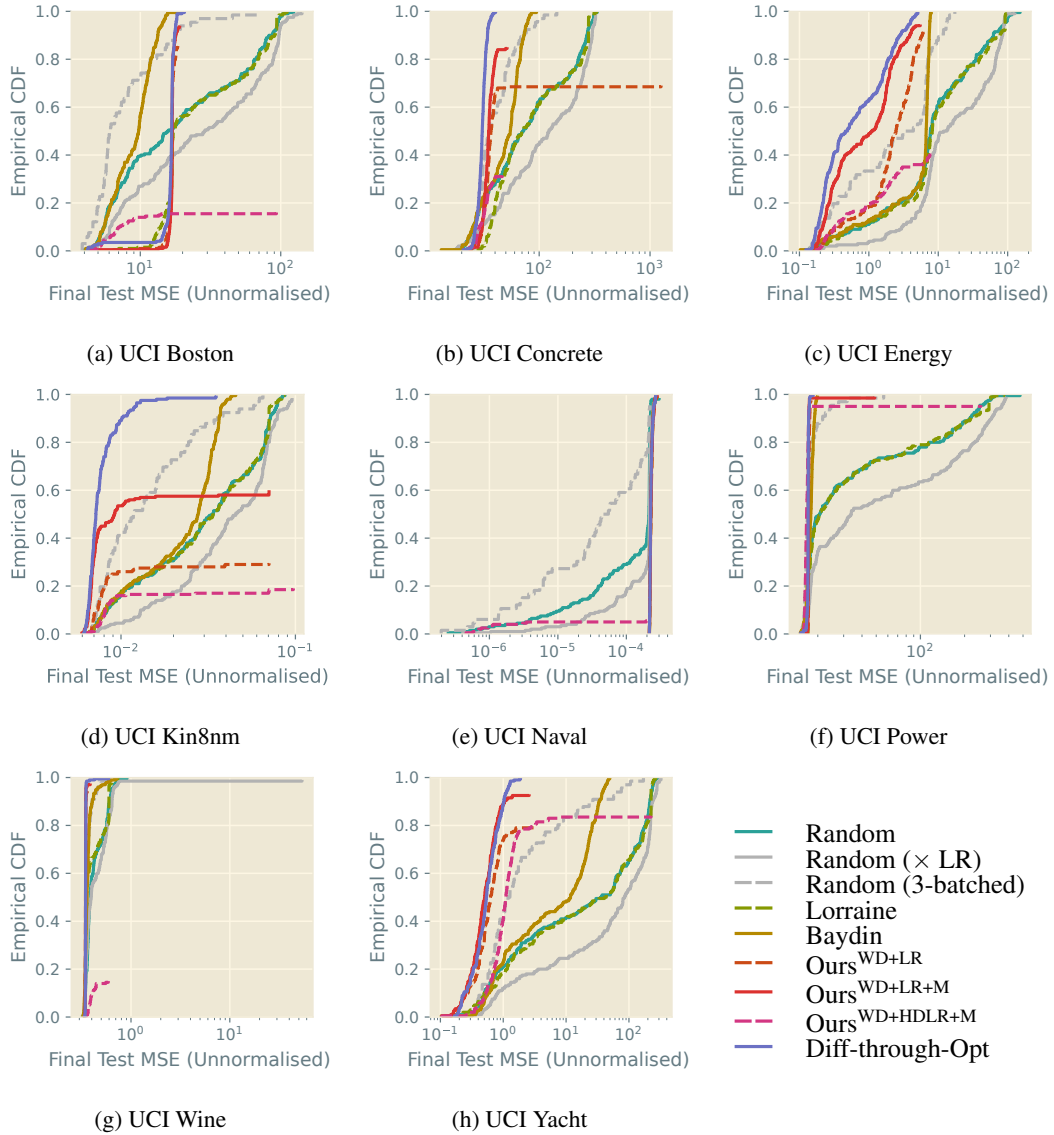


Figure 9: Empirical CDFs of final test losses, after training UCI datasets for 4 000 full-batch epochs from each of 200 random initialisations of SGD learning rate, weight decay and momentum. Runs ending with NaN losses account for the CDFs not reaching 1.0, and for the vertical lines to the right of the UCI Naval plot in (e). Higher curves are better; note the logarithmic horizontal scales.

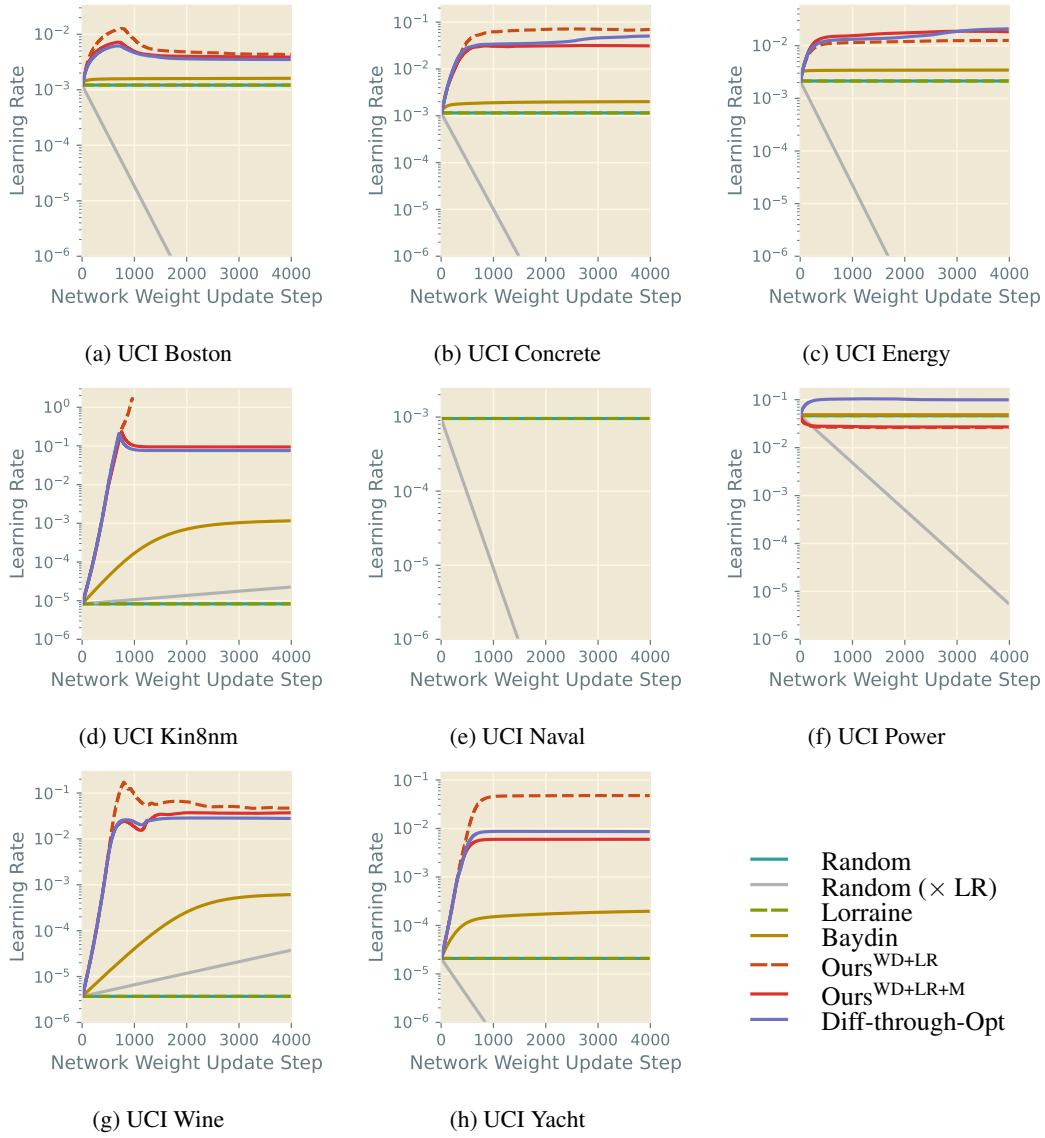


Figure 10: Sample learning rate evolutions after training UCI datasets for 4000 full-batch epochs; one of 200 random initialisations is shown for each dataset, chosen randomly from our results.

B.5 UCI AND FASHION-MNIST: BAYESIAN OPTIMISATION BASELINES

Table 6: Repeat of Table 1: final test MSE on selected UCI datasets. Now includes 36 repetitions of 30-sample Bayesian Optimisation, which is not considered in our emboldening.

Method	UCI Energy			UCI Kin8nm ($\times 1000$)			UCI Power		
	Mean	Median	Best	Mean	Median	Best	Mean	Median	Best
Random	21 \pm 2	7.8 \pm 0.4	0.120	38 \pm 2	33 \pm 3	6.44	67 \pm 6	21 \pm 2	15.4
Random (\times LR)	31 \pm 2	13 \pm 3	0.133	47 \pm 2	45 \pm 5	6.43	105 \pm 8	35 \pm 7	15.9
Random (3-batched)	4.5 \pm 0.6	4 \pm 2	0.141	18 \pm 2	13 \pm 1	6.72	19 \pm 2	17.1 \pm 0.2	15.5
Lorraine	22 \pm 2	8.2 \pm 0.5	0.161	38 \pm 2	34 \pm 3	6.39	67 \pm 6	21 \pm 1	16.4
Baydin	5.5 \pm 0.2	6.70 \pm 0.06	0.103	24.5 \pm 0.8	27 \pm 1	6.52	17.82 \pm 0.07	17.93 \pm 0.09	15.1
Ours ^{WD+LR}	2.5 \pm 0.1	2.2 \pm 0.2	0.147	10 \pm 1	7.6 \pm 0.1	6.44	17.33 \pm 0.01	17.27 \pm 0.01	15.5
Ours ^{WD+LR+M}	1.28 \pm 0.08	0.9 \pm 0.2	0.139	10 \pm 1	6.95 \pm 0.08	5.92	17.4 \pm 0.2	17.231 \pm 0.003	16.0
Ours ^{WD+HDLR+M}	1.9 \pm 0.2	1.2 \pm 0.3	0.165	16 \pm 4	8.1 \pm 0.1	6.29	18 \pm 1	16.76 \pm 0.04	16.0
Diff-through-Opt	1.10 \pm 0.09	0.48 \pm 0.09	0.123	8.0 \pm 0.2	7.17 \pm 0.06	6.09	17.17 \pm 0.02	17.193 \pm 0.005	15.3
Bayesian Optimisation	0.5 \pm 0.1	0.25 \pm 0.05	0.130	6.9 \pm 0.2	6.8 \pm 0.1	5.48	16.05 \pm 0.09	16.1 \pm 0.1	15.0

Table 7: Partial repeat of Table 2: final test cross-entropy on Fashion-MNIST. Now includes 36 repetitions of 30-sample Bayesian Optimisation, which is not considered in our emboldening.

Method	Fashion-MNIST		
	Mean	Median	Best
Random	0.85 \pm 0.07	0.51 \pm 0.05	0.334
Random (\times LR)	1.62 \pm 0.08	2.0 \pm 0.2	0.446
Random (3-batched)	0.8 \pm 0.1	0.5 \pm 0.1	0.351
Lorraine	0.87 \pm 0.07	0.52 \pm 0.05	0.343
Baydin	0.49 \pm 0.07	0.410 \pm 0.002	0.340
Ours ^{WD+LR}	0.375 \pm 0.002	0.375 \pm 0.003	0.336
Ours ^{WD+LR+M}	0.374 \pm 0.002	0.373 \pm 0.003	0.336
Ours ^{WD+HDLR+M}	0.402 \pm 0.004	0.389 \pm 0.003	0.358
Diff-through-Opt	0.388 \pm 0.001	0.387 \pm 0.002	0.359
Bayesian Optimisation	0.3502 \pm 0.0005	0.3500 \pm 0.0009	0.344

To contextualise our methods against the best possible performance, we also perform 32 repetitions of 30-sample Bayesian Optimisation (BO) on selected UCI datasets and Fashion-MNIST, using the same procedure as *Random* to train each sampled configuration (but now with an separate validation set used to compare configurations), and record these in Tables 6 and 7. We use the Python BO implementation of Nogueira (2014), retaining the default configuration that the first five of our 30 initialisations be drawn randomly from the space. All runtimes are measured based on 8-way parallel execution per GPU. Although BO involves a much greater computational burden than the other methods we consider, it should more robustly estimate the optimal hyperparameters.

Our average performance falls short of the BO benchmark, but we come substantially closer than the *Random* and *Lorraine* baselines, and similarly close as *Diff-through-Opt*. On Fashion-MNIST especially, our methods are very competitive, achieving performance in the vicinity of BO with 30 times less computation. Considering our best runs, we seem to suffer only a minor performance penalty (compared to the best hyperparameters we found) by adopting Algorithm 1.

As an additional comparison, we show in Figure 11 the evolution of incumbent best test loss over wall time during our previous training of 200 (UCI)/100 (Fashion-MNIST) initialisations. Clearly we would expect BO’s greater computation to result in smaller final losses, which we observe, but our methods are capable of reaching performant results much faster than BO. This underscores the principal benefit of our algorithm: with only a single training episode and a relatively small runtime penalty, we achieve a meaningful HPO effect, which reaches the vicinity of the ideal performance found by much slower and more computationally onerous methods.

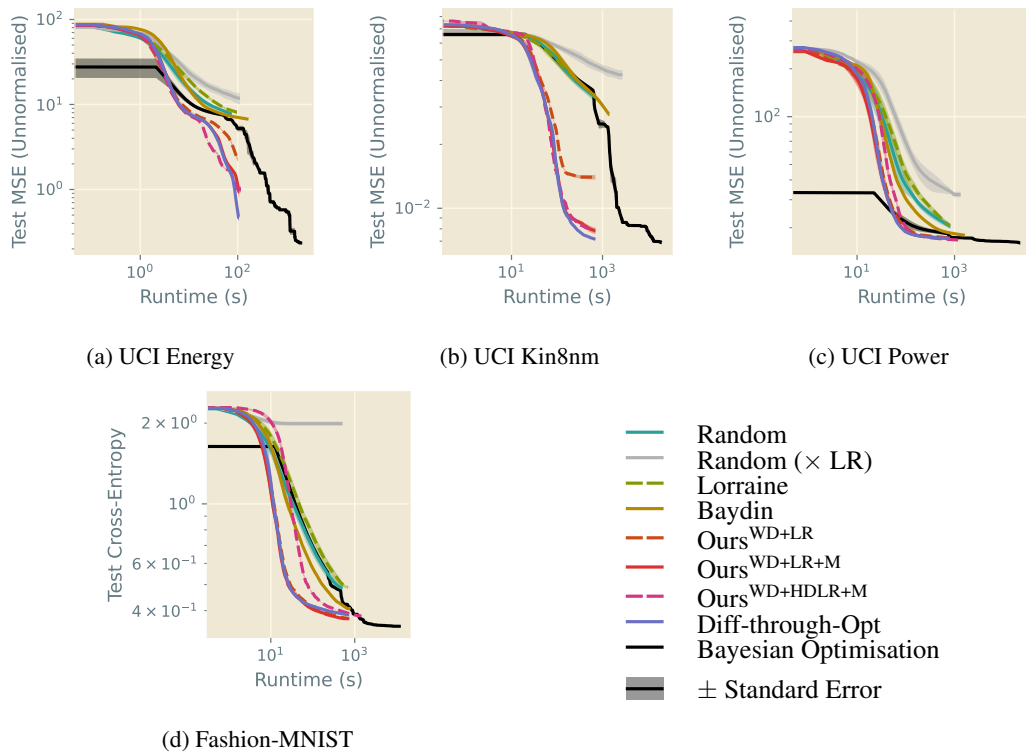
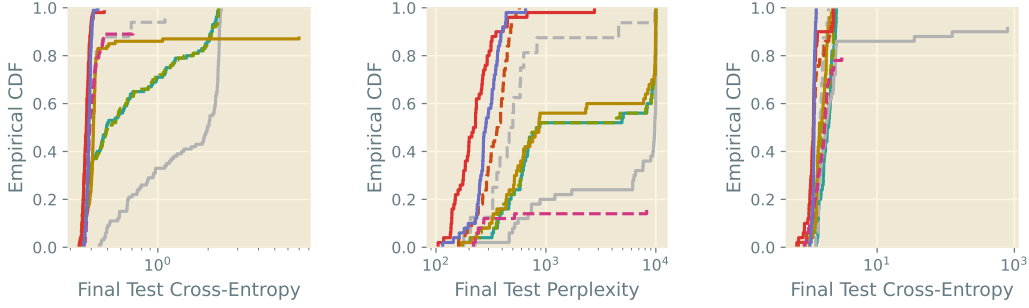


Figure 11: Evolution of incumbent best test MSE with time, during training of selected UCI datasets/Fashion-MNIST from 200/100 random hyperparameter initialisations, with Bayesian Optimisation for comparison. Shaded envelopes are bootstrapped standard errors of the best loss found at that time. Note the logarithmic horizontal axes.

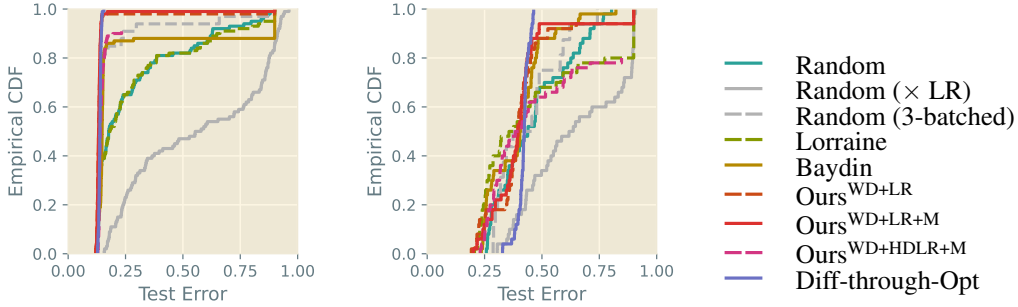
B.6 LARGE-SCALE DATASETS

For Fashion-MNIST, Penn Treebank and CIFAR-10, Figure 12 shows the empirical distributions of final test performance, contextualising the values shown in Table 2. In addition, Figure 13 and Table 8 show our results in terms of error percentages for Fashion-MNIST and CIFAR-10.



(a) Fashion-MNIST using an MLP (b) Penn Treebank using an LSTM (c) CIFAR-10 using a MobileNet-v2

Figure 12: Empirical CDFs of final test losses, trained on larger-scale datasets for $50^{(a)}/72^{(b,c)}$ epochs from $100^{(a)}/50^{(b,c)}$ random SGD hyperparameter initialisations. Key as in Figure 13; notes as in Figure 9.



(a) Fashion-MNIST using an MLP (b) CIFAR-10 using a MobileNet-v2

Figure 13: Empirical CDFs of final test errors after training on larger-scale datasets for $50^{(a)}/72^{(b)}$ epochs from each of $100^{(a)}/50^{(b)}$ random initialisations of SGD hyperparameters. Notes as in Figure 9.

Table 8: Quantitative analysis of final test errors from Figure 13. Bold values are the lowest in class.

Method	Fashion-MNIST			CIFAR-10		
	Mean	Median	Best	Mean	Median	Best
Random	0.28 ± 0.02	0.18 ± 0.02	0.116	0.46 ± 0.02	0.44 ± 0.03	0.245
Random (× LR)	0.56 ± 0.03	0.57 ± 0.09	0.157	0.64 ± 0.03	0.63 ± 0.07	0.261
Random (3-batched)	0.18 ± 0.02	0.135 ± 0.004	0.120	0.40 ± 0.03	0.38 ± 0.06	0.238
Lorraine	0.29 ± 0.02	0.19 ± 0.02	0.118	0.47 ± 0.04	0.37 ± 0.05	0.203
Baydin	0.24 ± 0.02	0.1480 ± 0.0007	0.118	0.40 ± 0.02	0.41 ± 0.02	0.219
Ours ^{WD+LR}	0.15 ± 0.01	0.1329 ± 0.0009	0.117	0.41 ± 0.02	0.395 ± 0.008	0.191
Ours ^{WD+LR+M}	0.141 ± 0.008	0.133 ± 0.001	0.118	0.40 ± 0.02	0.40 ± 0.01	0.196
Ours ^{WD+HDLR+M}	0.144 ± 0.001	0.1394 ± 0.0009	0.125	0.39 ± 0.02	0.34 ± 0.03	0.226
Diff-through-Opt	0.1384 ± 0.0005	0.1382 ± 0.0006	0.126	0.419 ± 0.004	0.423 ± 0.003	0.312

B.6.1 RUNTIMES

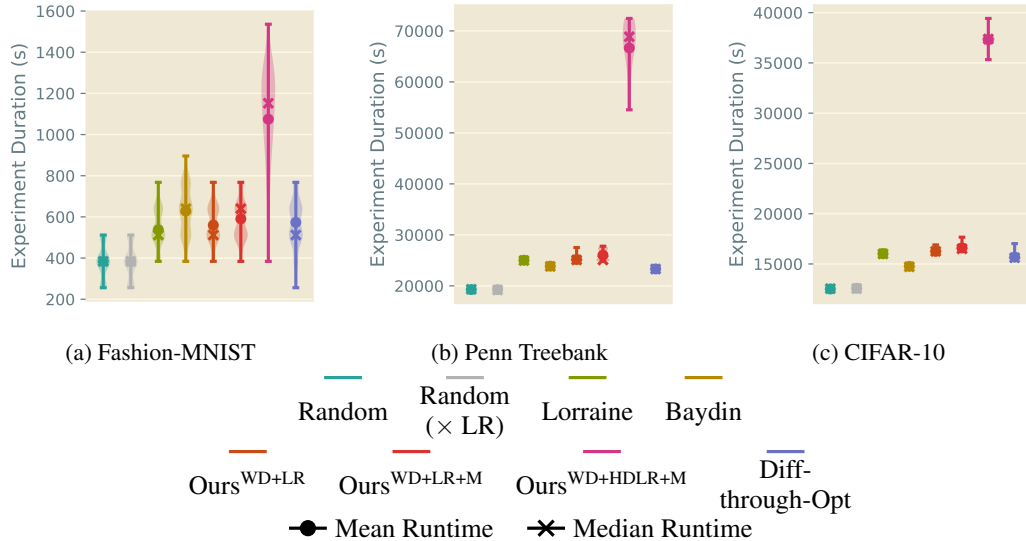


Figure 14: Single-pass runtime distributions for our larger-scale experiments. Worst-case complexities are dominated by second derivative computations, but remain competitive with conventional multi-pass HPO techniques, which scale our Random results by the number of configurations sampled.

For our larger-scale experiments, we illustrate comparative runtimes in Figure 14. More complex model architectures, with more learnable parameters, suffer a greater computational cost from taking second derivatives with respect to each model weight, which appears more prominently in our Penn Treebank and CIFAR-10 experiments. However, our extension of Lorraine et al. (2019)’s method to additional hyperparameters doesn’t dramatically increase runtimes: second derivative computations themselves are responsible for most added complexity. Even in the worst case (Fashion-MNIST), our scalar algorithms have similar runtimes to naïvely training two fixed hyperparameter initialisations (such as those considered by *Random*), comparing extremely favourably to HPO methods requiring repeated retraining. Naturally, the massive increase in the number of hyperparameters optimised by *Ours*^{WD+HDLR+M} causes a prominent jump in runtimes, but even this algorithm remains within a practical factor of the *Random* baseline.

B.6.2 BATCH NORMALISATION AND FASHION-MNIST

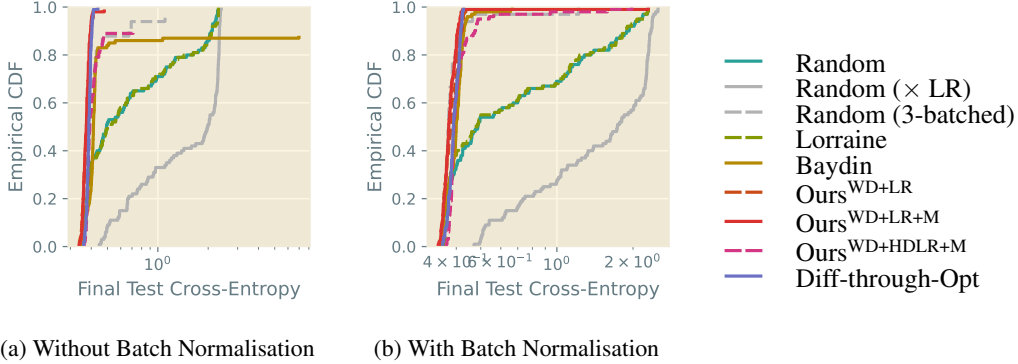


Figure 15: Comparing CDFs of final test cross-entropy from our Fashion-MNIST experiments of Section 4.2: (a) as before, without batch normalisation; (b) with batch normalisation in our simple MLP model.

Table 9: Quantitative analysis of final test cross-entropies from Figure 15 — investigating the use of batch normalisation on Fashion-MNIST. Bold values are the lowest in class.

Method	Without Batch Normalisation			With Batch Normalisation		
	Mean	Median	Best	Mean	Median	Best
Random	0.85 ± 0.07	0.51 ± 0.05	0.334	0.83 ± 0.06	0.50 ± 0.06	0.333
Random (× LR)	1.62 ± 0.08	2.0 ± 0.2	0.446	1.60 ± 0.07	1.7 ± 0.2	0.468
Random (3-batched)	0.8 ± 0.1	0.5 ± 0.1	0.351	0.46 ± 0.05	0.379 ± 0.009	0.341
Lorraine	0.87 ± 0.07	0.52 ± 0.05	0.343	0.82 ± 0.06	0.49 ± 0.06	0.342
Baydin	0.49 ± 0.07	0.410 ± 0.002	0.340	0.401 ± 0.005	0.400 ± 0.003	0.337
Ours ^{WD+LR}	0.375 ± 0.002	0.375 ± 0.003	0.336	0.383 ± 0.003	0.379 ± 0.003	0.337
Ours ^{WD+LR+M}	0.374 ± 0.002	0.373 ± 0.003	0.336	0.40 ± 0.02	0.374 ± 0.002	0.338
Ours ^{WD+HDLR+M}	0.402 ± 0.004	0.389 ± 0.003	0.358	0.44 ± 0.02	0.392 ± 0.002	0.354
Diff-through-Opt	0.388 ± 0.001	0.387 ± 0.002	0.359	0.392 ± 0.002	0.390 ± 0.002	0.351

As batch normalisation rescales the parameter gradients for each training step, it is capable of further influencing how final performance is governed by learning rates and their variations. To study this effect, we repeat the Fashion-MNIST experiments described in Section 4.2 using batch normalisation in our simple MLP model. Our results are plotted alongside the non-batch normalised CDFs in Figure 15, with averages summarised in Table 9.

Subjectively, performance does not seem to dramatically change when batch normalisation is invoked, with CDFs having broadly the same shape. Considering means and medians as our figures of merit (Table 9) suggests the same general pattern: generally, our algorithms benefit slightly from the absence of batch normalisation, and other algorithms benefit slightly from its presence, but there is not a unanimous trend. We conclude that, in the context of this work, batch normalisation does not substantially improve or hinder performance.

B.7 EFFECT OF SHORT-HORIZON BIAS

Attempts to quantify the effect of short-horizon bias in our experiments are frustrated by the need to perform computationally-intensive longer-horizon experiments, which has limited the scope of evaluations we can perform. However, we are able to study the potential improvements of longer horizons in three experimental settings.

B.7.1 TRUNCATED PROBLEM, FULL HORIZON

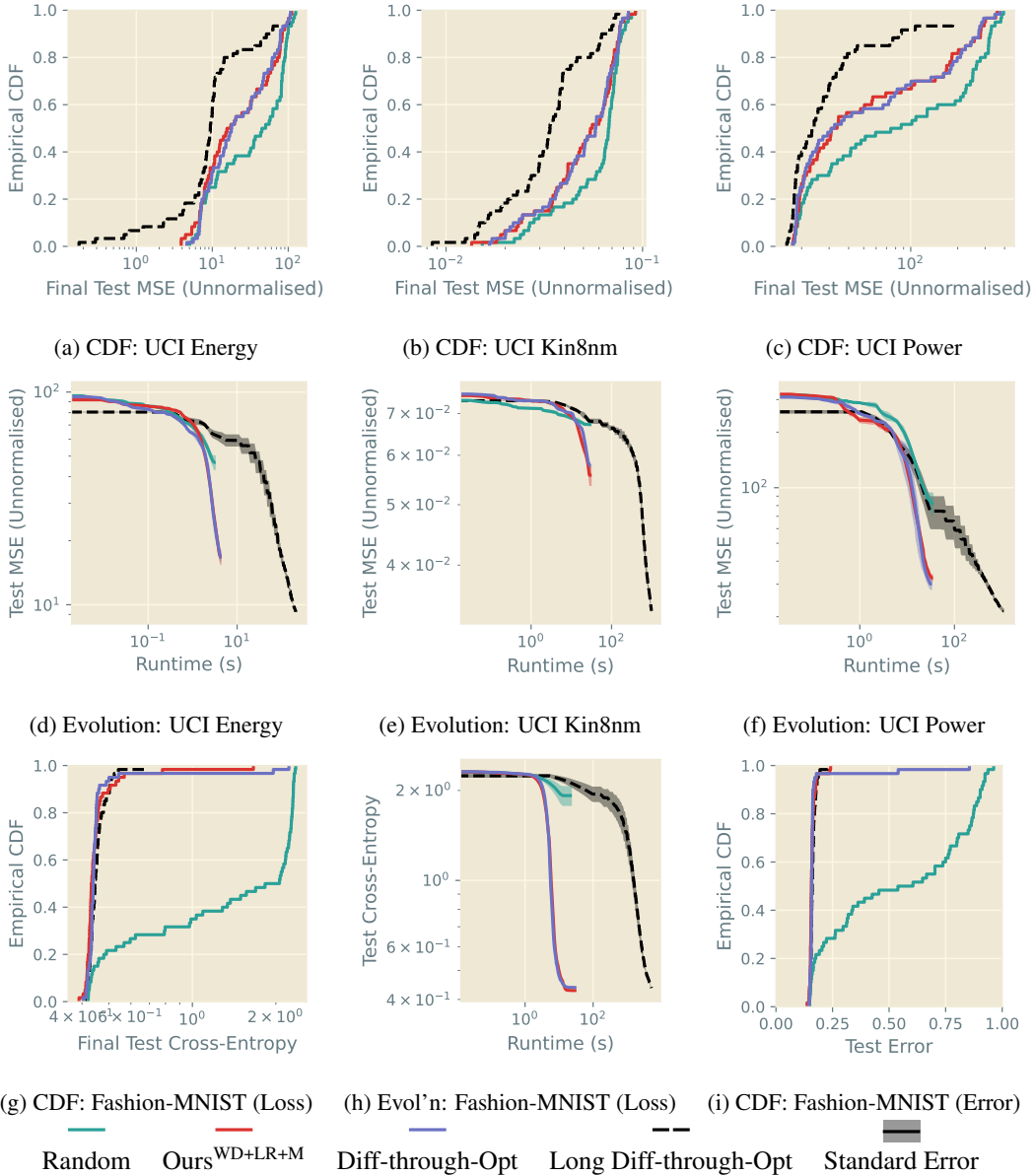


Figure 16: CDFs of final test losses and evolutions of bootstrapped median losses from 60 random initialisations on a shorter problem of 200 (UCI) / 1000 (Fashion-MNIST) network weight updates, featuring full-horizon *Long Diff-through-Opt* as described in Appendix B.7.1.

Firstly, we consider the four study datasets UCI Energy/Kin8nm/Power and Fashion-MNIST, shortening training so it only lasts for 200 (UCI) / 1000 (Fashion-MNIST) network weight update steps. This shorter training episode means we cannot compare to our results in Section 4, but does permit

Table 10: Quantitative analysis of UCI final test performance from Figure 16, including full-horizon *Long Diff-through-Opt* on shorter problems as described in Appendix B.7.1. Bold values are the lowest in class.

Method	UCI Energy			UCI Kin8nm ($\times 1\,000$)			UCI Power		
	Mean	Median	Best	Mean	Median	Best	Mean	Median	Best
Random	51 \pm 5	50 \pm 10	5.03	61 \pm 2	67 \pm 2	15.3	140 \pm 20	90 \pm 40	17.7
Ours ^{WD+LR+M}	35 \pm 4	19 \pm 7	3.89	54 \pm 2	56 \pm 5	13.5	90 \pm 10	30 \pm 10	17.5
Diff-through-Opt	34 \pm 4	20 \pm 6	4.61	54 \pm 2	57 \pm 5	16.6	100 \pm 10	40 \pm 10	17.5
Long Diff-through-Opt	16 \pm 3	9.3 \pm 0.5	0.145	37 \pm 2	34 \pm 2	8.47	32 \pm 4	23 \pm 2	16.1

Table 11: Quantitative analysis of Fashion-MNIST final test performance from Figure 16, including full-horizon *Long Diff-through-Opt* on a shorter problem as described in Appendix B.7.1. Bold values are the lowest in class.

Method	Final Test Cross-Entropy			Final Test Error		
	Mean	Median	Best	Mean	Median	Best
Random	1.5 \pm 0.1	1.8 \pm 0.3	0.409	0.54 \pm 0.04	0.6 \pm 0.1	0.145
Ours ^{WD+LR+M}	0.47 \pm 0.02	0.434 \pm 0.003	0.389	0.161 \pm 0.002	0.157 \pm 0.001	0.136
Diff-through-Opt	0.50 \pm 0.04	0.439 \pm 0.002	0.404	0.18 \pm 0.01	0.1582 \pm 0.0007	0.146
Long Diff-through-Opt	0.456 \pm 0.005	0.446 \pm 0.004	0.396	0.163 \pm 0.002	0.160 \pm 0.001	0.141

full-horizon differentiation-through-optimisation. *Long Diff-through-Opt* does exactly this, performing 30 (UCI) / 50 (Fashion-MNIST) hyperparameter updates using the maximum look-back horizon and restarting training with the new hyperparameters after each update. In this sense, we use 30 or 50 times as much computation as in our other algorithms (here: *Random*, *Ours*^{WD+LR+M} and *Diff-through-Opt*). The latter update their hyperparameters at the same intervals as before, giving 20 (UCI) / 100 (Fashion-MNIST) updates overall. We take 60 random hyperparameter initialisations and run each of these four methods on them.

Our results are shown in Figure 16 and Tables 10 and 11. They show a stark contrast between datasets — on UCI trials, *Long Diff-through-Opt* manages, as expected, to achieve substantially improved final performance over its short-horizon competition, but on Fashion-MNIST, performance is much more similar between HPO algorithms. Wu et al. (2018) intuit short-horizon bias by describing the simple setting of a quadratic with different curvature magnitudes in each dimension, and we expect the simpler UCI datasets to match this clean depiction of the optimisation space more closely than Fashion-MNIST. Thus, we speculate the space of non-trivial datasets, such as Fashion-MNIST, is sufficiently complicated that merely eliminating short-horizon bias is insufficient to prevent the optimiser from getting stuck in similarly-performant local optima.

B.7.2 FASHION-MNIST, MEDIUM HORIZON

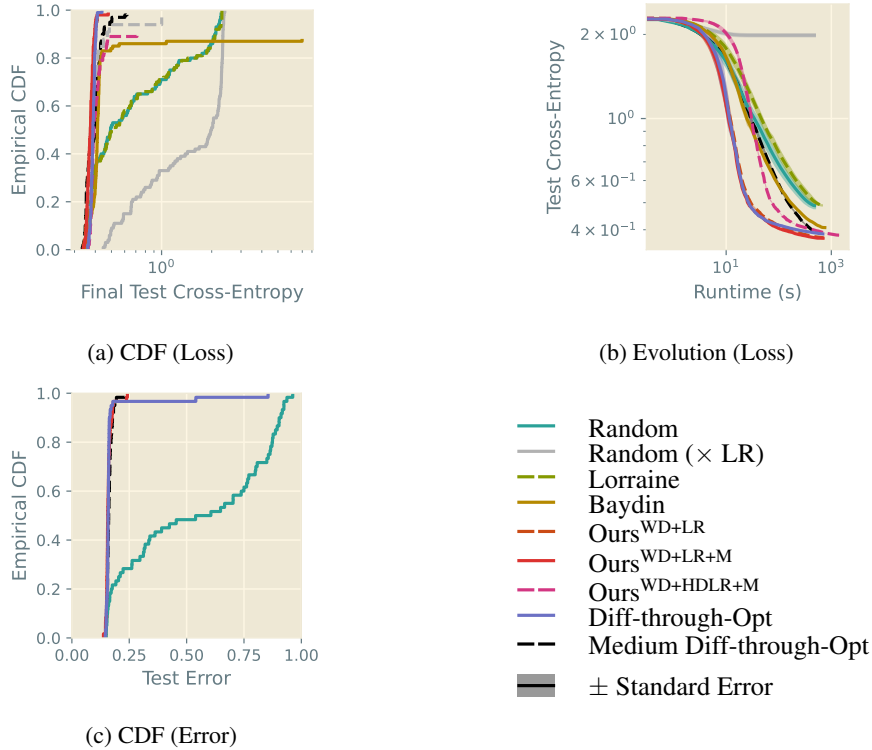


Figure 17: CDFs of final test losses and evolutions of bootstrapped median losses from 100 random initialisations on Fashion-MNIST, featuring *Medium Diff-through-Opt* with a 200-step look-back horizon as described in Appendix B.7.2.

Table 12: Quantitative analysis of Fashion-MNIST final test performance from Figure 17, including *Medium Diff-through-Opt* with a 200-step look-back horizon as described in Appendix B.7.2. Bold values are the lowest in class.

Method	Final Test Cross-Entropy			Final Test Error		
	Mean	Median	Best	Mean	Median	Best
Random	0.85 ± 0.07	0.51 ± 0.05	0.334	0.28 ± 0.02	0.18 ± 0.02	0.116
Random (× LR)	1.62 ± 0.08	2.0 ± 0.2	0.446	0.56 ± 0.03	0.57 ± 0.09	0.157
Random (3-batched)	0.8 ± 0.1	0.5 ± 0.1	0.351	0.18 ± 0.02	0.135 ± 0.004	0.120
Lorraine	0.87 ± 0.07	0.52 ± 0.05	0.343	0.29 ± 0.02	0.19 ± 0.02	0.118
Baydin	0.49 ± 0.07	0.410 ± 0.002	0.340	0.24 ± 0.02	0.1480 ± 0.0007	0.118
Ours ^{WD+LR}	0.375 ± 0.002	0.375 ± 0.003	0.336	0.15 ± 0.01	0.1329 ± 0.0009	0.117
Ours ^{WD+LR+M}	0.374 ± 0.002	0.373 ± 0.003	0.336	0.141 ± 0.008	0.133 ± 0.001	0.118
Ours ^{WD+HDLR+M}	0.402 ± 0.004	0.389 ± 0.003	0.358	0.144 ± 0.001	0.1394 ± 0.0009	0.125
Diff-through-Opt	0.388 ± 0.001	0.387 ± 0.002	0.359	0.1384 ± 0.0005	0.1382 ± 0.0006	0.126
Medium Diff-through-Opt	0.395 ± 0.005	0.396 ± 0.007	0.332	0.148 ± 0.008	0.141 ± 0.003	0.117

Next, we note our Fashion-MNIST experiments of Section 4 run for 10 000 network weight steps, which can accommodate a longer look-back horizon for the purposes of our study. We introduce a new algorithm, *Medium Diff-through-Opt*, which is identical to our previous Fashion-MNIST *Diff-through-Opt* configuration, except the look-back horizon is now 200 steps, and the number of hyperparameter updates reduced to 50 to keep the same computational burden. This setting explores the trade-off between hypergradient accuracy and number of hypergradients computed. We apply this new configuration to the same 100 iterations as before, plotting combined results in Figure 17 and Table 12.

Again, we see that Fashion-MNIST seems resilient to the short-horizon bias, with this medium-horizon configuration unable to substantially improve on our existing results. Naturally, since *Medium Diff-through-Opt* performs fewer hyperparameter updates, its performance may suffer if the hyperparameters have not converged, which we expect to be the likely cause here. However, it is reassuring that our methods are capable of performing well despite their short-horizon basis.

B.7.3 UCI ENERGY, FULL HORIZON

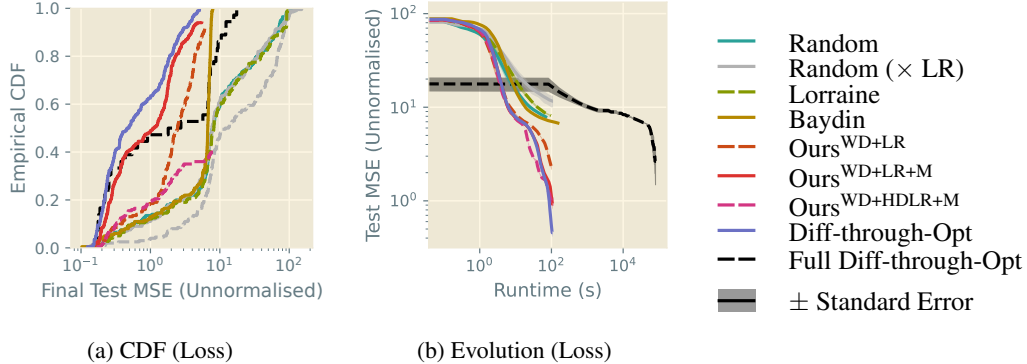


Figure 18: CDF of final test losses and evolution of bootstrapped median losses from 200 random initialisations on UCI Energy, featuring 36 initialisations of *Full Diff-through-Opt* with a 4 000-step look-back horizon as described in Appendix B.7.3.

Table 13: Quantitative analysis of UCI Energy final test performance from Figure 18, including *Full Diff-through-Opt* with a 4 000-step look-back horizon as described in Appendix B.7.3. Bold values are the lowest in class.

Method	Final Test MSE				
	Mean		Median		Best
Random	21	± 2	7.8	± 0.4	0.120
Random (× LR)	31	± 2	13	± 3	0.133
Random (3-batched)	4.5	± 0.6	4	± 2	0.141
Lorraine	22	± 2	8.2	± 0.5	0.161
Baydin	5.5	± 0.2	6.70	± 0.06	0.103
Ours ^{WD+LR}	2.5	± 0.1	2.2	± 0.2	0.147
Ours ^{WD+LR+M}	1.28	± 0.08	0.9	± 0.2	0.139
Ours ^{WD+HDLR+M}	1.9	± 0.2	1.2	± 0.3	0.165
Diff-through-Opt	1.10	± 0.09	0.48	± 0.09	0.123
Full Diff-through-Opt	4.7	± 0.8	3	± 2	0.129

Finally, we consider UCI Energy, whose size is more amenable to full-horizon studies. Our new setting here, *Full Diff-through-Opt*, extends the *Diff-through-Opt* configuration from Section 4 by using a full look-back horizon of 4 000 steps, restarting training after each hyperparameter update and performing 30 such updates. This permits a full-horizon study on the same problem as before, using a similar computational footprint to our Bayesian Optimisation trials of Appendix B.5 (that is, 30 times the cost of our original experiments). We consider 32 random initialisations for this algorithm, and combine the results with our original UCI Energy experiments, showing both in Figure 18 and Table 13.

Curiously, while *Full Diff-through-Opt* outclasses naïve *Random* approaches, it is very uncompetitive with its short-horizon counterparts, achieving much higher average final losses (the larger variance being, of course, expected due to the smaller number of repetitions). The principal difference between *Full Diff-through-Opt* and *Diff-through-Opt*, apart from the different look-back distances, is the number of hyperparameter updates performed, since these are far more expensive in the former case. While more hyperparameter updates would likely cause *Full Diff-through-Opt*’s performance to improve, the computational impact would be massive, with such a setting unlikely to be desired in practical applications. Again, we conclude that it is simplistic to claim short-horizon bias renders an algorithm ill-suited to HPO — in reality, it is one of many factors worthy of consideration in the selection of an approach. In this case, the larger number of updates we are able to perform by sacrificing horizon length leads to favourable performance improvements, even though this optimisation is technically ‘biased’ as a result.

C COMPLETE DERIVATION

Here, we reprise the derivations of Section 2 in more verbose form. Our subsections mirror those used previously.

C.1 IMPLICIT FUNCTION THEOREM IN BILEVEL OPTIMISATION

Recall that we consider some model parameterised by parameters \mathbf{w} , which we train to minimise a training loss \mathcal{L}_T . Our training algorithm is governed by hyperparameters λ , which we simultaneously train to minimise a validation loss \mathcal{L}_V . We target optimal \mathbf{w}^* and λ^* , defined by the *bilevel optimisation problem*

$$^{(a)} \lambda^* = \arg \min_{\lambda} \mathcal{L}_V(\lambda, \mathbf{w}^*(\lambda)), \quad \text{such that} \quad ^{(b)} \mathbf{w}^*(\lambda) = \arg \min_{\mathbf{w}} \mathcal{L}_T(\lambda, \mathbf{w}). \quad (1 \text{ revisited})$$

(1b) simply reflects a standard model training procedure, with fixed λ , so we need only consider how to choose the λ^* from (1a).

Suppose we seek a gradient-based hyperparameter optimisation method for its performance potential. We then require the total derivative of the validation objective \mathcal{L}_V with respect to the hyperparameters λ , which may be obtained by the chain rule:

$$\frac{d\mathcal{L}_V}{d\lambda} = \frac{\partial \mathcal{L}_V}{\partial \lambda} + \frac{\partial \mathcal{L}_V}{\partial \mathbf{w}^*} \frac{\partial \mathbf{w}^*}{\partial \lambda}. \quad (2 \text{ revisited})$$

An exact expression for $\frac{\partial \mathbf{w}^*}{\partial \lambda}$ can be obtained by applying Cauchy’s Implicit Function Theorem (Theorem 1). Suppose that for some λ' we have identified a locally optimal \mathbf{w}' , and assume continuous differentiability of $\frac{\partial \mathcal{L}_T}{\partial \mathbf{w}}$. Then, there exists an open subset of hyperparameter space containing λ' , over which we can define a function $\mathbf{w}^*(\lambda)$ relating locally optimal \mathbf{w} for each λ by

$$\frac{\partial \mathbf{w}^*}{\partial \lambda} = - \left(\frac{\partial^2 \mathcal{L}_T}{\partial \mathbf{w} \partial \mathbf{w}^\top} \right)^{-1} \frac{\partial^2 \mathcal{L}_T}{\partial \mathbf{w} \partial \lambda^\top}. \quad (3 \text{ revisited})$$

Of course, the inverse Hessian term in (3) becomes rapidly intractable for models at realistic scale.

C.2 APPROXIMATE BEST-RESPONSE DERIVATIVE

To proceed, we require an approximate expression for $\frac{\partial \mathbf{w}^*}{\partial \lambda}$. Suppose model training proceeds iteratively by the rule

$$\mathbf{w}_i(\lambda) = \mathbf{w}_{i-1}(\lambda) - \mathbf{u}(\lambda, \mathbf{w}_{i-1}(\lambda)), \quad (4 \text{ revisited})$$

where i is the current iteration and \mathbf{u} is an arbitrary function differentiable in both its arguments. Note that the trivial choice

$$\mathbf{u}(\lambda, \mathbf{w}_{i-1}(\lambda)) = \mathbf{w}_{i-1}(\lambda) - \mathbf{f}(\lambda, \mathbf{w}_{i-1}(\lambda)) \quad (8)$$

allows arbitrary differentiable weight updates \mathbf{f} to be subsumed by this framework.

Differentiating with respect to λ at the current hyperparameters λ' , we have:

$$\left[\frac{\partial \mathbf{w}_i}{\partial \lambda} \right]_{\lambda'} = \left[\frac{\partial \mathbf{w}_{i-1}}{\partial \lambda} \right]_{\lambda'} - \left[\frac{d\mathbf{u}}{d\lambda} \right]_{\lambda', \mathbf{w}_{i-1}(\lambda')} \quad (9)$$

$$= \left[\frac{\partial \mathbf{w}_{i-1}}{\partial \lambda} \right]_{\lambda'} - \left[\frac{\partial \mathbf{u}}{\partial \mathbf{w}} \frac{\partial \mathbf{w}_{i-1}}{\partial \lambda} + \frac{\partial \mathbf{u}}{\partial \lambda} \right]_{\lambda', \mathbf{w}_{i-1}(\lambda')} \quad (10)$$

$$= \left[\left(\mathbf{I} - \frac{\partial \mathbf{u}}{\partial \mathbf{w}} \right) \frac{\partial \mathbf{w}_{i-1}}{\partial \lambda} - \frac{\partial \mathbf{u}}{\partial \lambda} \right]_{\lambda', \mathbf{w}_{i-1}(\lambda')} \quad (11)$$

$$= - \left[\frac{\partial \mathbf{u}}{\partial \lambda} \right]_{\lambda', \mathbf{w}_{i-1}(\lambda')} + \left[\mathbf{I} - \frac{\partial \mathbf{u}}{\partial \mathbf{w}} \right]_{\lambda', \mathbf{w}_{i-1}(\lambda')} \left[\left(\mathbf{I} - \frac{\partial \mathbf{u}}{\partial \mathbf{w}} \right) \frac{\partial \mathbf{w}_{i-2}}{\partial \lambda} - \frac{\partial \mathbf{u}}{\partial \lambda} \right]_{\lambda', \mathbf{w}_{i-2}(\lambda')} \quad (12)$$

$$= - \sum_{0 \leq j < i} \left(\left(\prod_{0 \leq k \leq j} \left[\mathbf{I} - \frac{\partial \mathbf{u}}{\partial \mathbf{w}} \right]_{\lambda', \mathbf{w}_{i-1-k}(\lambda')} \right) \left[\frac{\partial \mathbf{u}}{\partial \lambda} \right]_{\lambda', \mathbf{w}_{i-1-j}(\lambda')} \right) \quad (5 \text{ revisited})$$

To combine terms in (5), we must make approximations such that all bracketed expressions are evaluated at the same λ, \mathbf{w} . For network weights \mathbf{w} , we set $\mathbf{w}_0 = \mathbf{w}_i = \mathbf{w}^*$ for all iterations i , effectively assuming we have been at the optimal \mathbf{w} for some time; when we come to consider finite truncations of the summation, this approximation will be especially appealing. With this approximation, we may collapse the product and write

$$\left[\frac{\partial \mathbf{w}_i}{\partial \lambda} \right]_{\lambda'} \approx - \sum_{j < i} \left[\left(\prod_{k \leq j} \left(\mathbf{I} - \frac{\partial \mathbf{u}}{\partial \mathbf{w}} \right) \right) \frac{\partial \mathbf{u}}{\partial \lambda} \right]_{\lambda', \mathbf{w}^*(\lambda')} \quad (13)$$

$$= - \left[\sum_{0 \leq j < i} \left(\mathbf{I} - \frac{\partial \mathbf{u}}{\partial \mathbf{w}} \right)^j \frac{\partial \mathbf{u}}{\partial \lambda} \right]_{\lambda', \mathbf{w}^*(\lambda')} . \quad (6 \text{ revisited})$$

As i increases, our training algorithm should converge towards a locally optimal \mathbf{w}^* , and the summation in (6) will accrue more terms. Instead, we reinterpret i as specifying the finite number of terms we consider as an approximation to the whole sum. With this redefined i , we arrive at our approximate best-response Jacobian

$$\left[\frac{\partial \mathbf{w}^*}{\partial \lambda} \right]_{\lambda'} \approx - \left[\sum_{j < i} \left(\mathbf{I} - \frac{\partial \mathbf{u}}{\partial \mathbf{w}} \right)^j \frac{\partial \mathbf{u}}{\partial \lambda} \right]_{\lambda', \mathbf{w}^*(\lambda')} . \quad (6 \text{ revisited})$$

C.3 CONVERGENCE TO BEST-RESPONSE DERIVATIVE

To informally argue the convergence properties of our method, note that (6) is a truncated Neumann series:

$$\left[\frac{\partial \mathbf{w}_i}{\partial \lambda} \right]_{\lambda'} \approx - \left[\sum_{j < i} \left(\mathbf{I} - \frac{\partial \mathbf{u}}{\partial \mathbf{w}} \right)^j \frac{\partial \mathbf{u}}{\partial \lambda} \right]_{\lambda', \mathbf{w}^*(\lambda')} . \quad (14)$$

Analogously to its scalar equivalent — the geometric series — this series converges as $i \rightarrow \infty$ if the multiplicative term $(\mathbf{I} - \frac{\partial \mathbf{u}}{\partial \mathbf{w}})$ is ‘contractive’ in some sense. For our purposes, it suffices to assume a Banach space and, for the operator norm $\|\cdot\|$, that $\|\mathbf{I} - \frac{\partial \mathbf{u}}{\partial \mathbf{w}}\| < 1$. In this case, we can directly apply the closed-form limit expression for the Neumann series:

$$\lim_{i \rightarrow \infty} \left[\frac{\partial \mathbf{w}_i}{\partial \lambda} \right]_{\lambda'} \approx - \lim_{i \rightarrow \infty} \left[\sum_{j < i} \left(\mathbf{I} - \frac{\partial \mathbf{u}}{\partial \mathbf{w}} \right)^j \frac{\partial \mathbf{u}}{\partial \lambda} \right]_{\lambda', \mathbf{w}^*(\lambda')} \quad (15)$$

$$= - \left[\left(\mathbf{I} - \left(\mathbf{I} - \frac{\partial \mathbf{u}}{\partial \mathbf{w}} \right) \right)^{-1} \frac{\partial \mathbf{u}}{\partial \lambda} \right]_{\lambda', \mathbf{w}^*(\lambda')} \quad (16)$$

$$= - \left[\left(\frac{\partial \mathbf{u}}{\partial \mathbf{w}} \right)^{-1} \frac{\partial \mathbf{u}}{\partial \lambda} \right]_{\lambda', \mathbf{w}^*(\lambda')} . \quad (7 \text{ revisited})$$

Note that (7) is exactly the result of the Implicit Function Theorem (3) applied to our more general weight update \mathbf{u} . Concretely, suppose for some λ'' and \mathbf{w}'' that $\mathbf{u}(\lambda'', \mathbf{w}'') = \mathbf{0}$; in words, that our training process does not update the network weights at this point in weight-hyperparameter space, and assume \mathbf{u} is continuously differentiable with invertible Jacobian. Then, over some subset of hyperparameter space containing λ'' , we can say: $\mathbf{w}^*(\lambda)$ exists, we have $\mathbf{u}(\lambda, \mathbf{w}^*(\lambda)) = \mathbf{0}$ throughout the subspace and $\frac{\partial \mathbf{w}^*}{\partial \lambda}$ is given by (7) exactly.

C.4 SUMMARY OF DIFFERENCES FROM LORRAINE ET AL. (2019)

In their derivation, which ours closely parallels, Lorraine et al. (2019) replace (4) with a hard-coded SGD update step; in our notation, they fix $\mathbf{u}(\lambda, \mathbf{w}) = \mathbf{u}_{\text{SGD}}(\lambda, \mathbf{w}) = \eta \frac{\partial \mathcal{L}_T}{\partial \mathbf{w}}$. They then isolate the

learning rate η , insisting all hyperparameters λ must be dependent variables of the training loss \mathcal{L}_T , before further differentiating the training loss in their derivation. Consequently, their algorithm cannot optimise optimiser hyperparameters such as learning rates and momentum factors, since these come into play only *after* the training loss has been computed and differentiated.

Instead, we define a *general* weight update step (4), without assuming any particular form. We may then differentiate the general update \mathbf{u} directly, encompassing any hyperparameters appearing within it but outside the training loss, which Lorraine et al. (2019) would miss. Crucially, this includes the hyperparameters of most gradient-based optimisers, including SGD. Thus, we lift Lorraine et al.'s results from expressions about $\frac{\partial \mathcal{L}_T}{\partial \mathbf{w}}$ to expressions about \mathbf{u} , then update hyperparameters inaccessible to the former. Concretely: we optimise weight decay coefficients, learning rates and momentum factors in settings where Lorraine et al. can only manage the weight decay alone.